Accepted Manuscript

Design, synthesis and evaluation of novel 2-amino-3-(naphth-2-yl)propanoic acid derivatives as potent inhibitors of platelet aggregation

Zhouling Xie, Benimana Oscar, Lulu Zhao, Xue Ding, Chen Cao, Sen Feng, Han Li, Chen Pan, Ziyi Bian, Yang Li, Weijun Wang, Yi Kong, Zhiyu Li

PII: S0223-5234(16)30762-0

DOI: 10.1016/j.ejmech.2016.09.032

Reference: EJMECH 8898

To appear in: *European Journal of Medicinal Chemistry*

Received Date: 18 May 2016

Revised Date: 4 September 2016

Accepted Date: 9 September 2016

Please cite this article as: Z. Xie, B. Oscar, L. Zhao, X. Ding, C. Cao, S. Feng, H. Li, C. Pan, Z. Bian, Y. Li, W. Wang, Y. Kong, Z. Li, Design, synthesis and evaluation of novel 2-amino-3-(naphth-2-yl)propanoic acid derivatives as potent inhibitors of platelet aggregation, *European Journal of Medicinal Chemistry* (2016), doi: 10.1016/j.ejmech.2016.09.032.

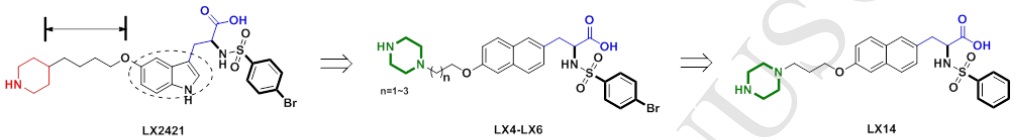

Two fold less potent than Tirofiban in antiplatelet aggregation (IC_{50}= 0.18 μM vs IC_{50}= 0.09 μM)

Two fold less potent than Tirofiban in inhibiting GPIIb/IIIa receptor (IC_{50}= 0.08 μM vs IC_{50}= 0.04 μM)

Lower bleeding risk than Tirofiban

Design, synthesis and evaluation of novel 2-amino-3-(naphth-2-yl)propanoic acid derivatives as potent inhibitors of platelet aggregation

Zhouling Xie[a], Benimana Oscar[a], Lulu Zhao[a], Xue Ding[b], Chen Cao[a], Sen Feng[a], Han Li[a], Chen Pan[a], Ziyi Bian[a], Yang Li[a], Weijun Wang [a], Yi Kong[b]**, Zhiyu Li[a]*

[a]*Jiangsu Key Laboratory of Drug Design and Optimization, China Pharmaceutical University, Nanjing 21009, China*

[b]*School of Life Science & Technology, China Pharmaceutical University, 24 Tongjiaxiang, Nanjing 210009, P.R.China*

E-mail addresses: zhiyuli@cpu.edu.cn (Z. Li), yikong668@163.com (Y. Kong)

Abstract: Based upon **LX2421**, a previously identified antiplatelet aggregation agent, a series of novel 2-amino-3-(naphth-2-yl)propanoic acid derivatives were designed, synthesized and evaluated. Among them, compounds **LX14** and **LX25** were identified as promising antiplatelet aggregation agents. The *in vitro* biologic study demonstrated that **LX14** can block platelet aggregation induced by four different inducers and displays comparable potency in inhibiting GPIIb/IIIa receptor in comparison with **Tirofiban**. In addition, **LX14** has much lower risk of bleeding than **Tirofiban** and shows significant antithrombotic activity *in vivo*. Taking together, the results indicated that **LX14** is a promising GPIIb/IIIa receptor antagonist against platelet aggregation worthy of further evaluation.

Key words: antiplatelet aggregation, GPIIb/IIIa receptor, inhibitor, naphthalene derivatives, antithrombotic activity, bleeding risk

1. Introduction

Coronary artery thrombosis diseases, such as myocardial infarction, acute coronary syndrome, and pulmonary embolism, represent the most frequent cause of mortality and morbidity worldwide [1-3]. Platelets are primary components for the development of thrombotic disorders. They can be activated by a number of platelet inducers, including Von Willebrand factor, collagens, fibronectin, vitronectin (VIN), adenosine 5′-diphosphate (ADP), thrombin, platelet activating factor (PAF), and epinephrine (EPN), which are released to arterial circulation on account of plaque rupture [4, 5]. Activated platelets also can produce activating molecules, such as like thromboxane A2 (TXA2) and ADP, further causing platelets shape change, secretion and increasing of the expression of GPIIb/IIIa receptor [6-9].

After platelet activation, GPIIb/IIIa receptors are exposed and activated to combine with the Arg-Gly-Asp (RGD) sequence of fibrinogen [10, 11]. One molecule of fibrinogen can bind to several platelets and one platelet can also combine with multiple fibrinogens [12]. Ultimately, this so called "cross-linking effect" leads to formation of thrombus which overwhelms the luminal area of the vessel, and causes various thrombotic diseases. Activation of GPIIb/IIIa receptor is the final common pathway of platelet aggregation regardless of the initiating inducer molecules, thus blocking the platelet GPIIb/IIIa receptor could effectively inhibit platelet aggregation (**Figure 1**) [13, 14].

Currently, three classes of antiplatelet aggregation drugs are frequently used in clinic: 1) aspirin, which blocks the production of the platelet activating molecule TXA2 by inhibiting the cyclooxygenase pathway [15]; 2) clopidogrel and prasugrel, which function as antagonists of the cell-surface ADP receptor $P2Y_{12}$ [16] and 3) the GPIIb/IIIa receptor antagonists, such as Abciximab, Eptifibatide and Tirofiban [17]. In clinical application the efficacy of aspirin and $P2Y_{12}$ receptors is limited by their restricted spectrum of antiplatelet activity, because platelets can be activated by several other inducers. This promotes the development of potent inhibitors of platelet aggregation based on the inhibition of GPIIb/IIIa [18]. Among the GPIIa/IIIb receptor antagonists, Abciximab is a non-competitive antagonist of GPIIb/IIIa which also interacts with two other intergrins $\alpha_v\beta_3$ and $\alpha_M\beta_2$, while Eptifibatide and Tirofiban mimicking the RGD sequence of fibrinogen are selective and competitive antagonists of GPIIb/IIIa [19]. The GPIIb/IIIa inhibitors have proven effectiveness in reducing the risk of periprocedural myocardial infraction (PMI) and urgently target vessel revascularization during catheterization. However, they also have several limitations, such as the risk of bleeding and the induction of thrombocytopenia in some patients [20], therefore, novel GPIIb/IIIa inhibitors with reduced risks are urgently needed.

In our previous efforts to discover novel antiplatelet agents, a series of tryptophan derivatives were designed and synthesized based on a three mer peptide pENW derived from Agkistrodon acutus Guenther venom [21, 22]. Among them, **LX2421** was the most potent compound which inhibits platelet aggregation induced by all of the four agonists (ADP, Thrombin, U46619 and Collagen). It has an IC_{50} value of 24.8 μM in an assay using ADP-induced rabbit platelet-rich plasma and shows moderate GPIIb/IIIa receptor inhibitory activity with an IC_{50} value of 5.4 μM, as potent as the known GPIIb/IIIa receptor antagonist, RGDs [23]. In addition, **LX2421** has much lower bleeding risk than **Tirofiban** and remarkable antithrombotic activity in arterial and venous thrombosis models in rats. Overall, **LX2421** is a promising lead for continuous study. In this paper, we reported the design, synthesis and evaluation of a novel series of 2-amino-3-(naphth-2-yl)propanoic acid derivatives with the purpose to improve further the antiplatelet aggregation activity and to reduce the bleeding risk by structural modifications

of **LX2421**.

2. Result and Discussion

2.1 Design and Structure-Activity Relationship

In order to explore the binding mode of **LX2421** to GPIIb/IIIa, we have performed molecular docking for its interaction with GPIIb/IIIa using the crystal structure of GPIIb/IIIa in complex with **Tirofiban** (PDB CODE: 2VDM, **Figure 2**). Our results indicated that there are multiple interactions between **LX2421** and GPIIb/IIIa. The 4-piperidyl group in **LX2421** has a salt bridge interaction with the carboxyl group of the Asp224 residue in GPIIb subunit, while the carboxyl group forms several hydrogen bonds with Ser123, Asn215 residues and also has interaction with the MIDAS Mg^{2+} ion of GPIIIa. The indole ring has π-π interaction with the phenyl ring of Tyr190. To fully understand the binding mode and key interactions of **LX2421** and GPIIb/IIIa, molecular dynamics (MD) simulations were carried out. The binding interactions between **LX2421** and GPIIb/IIIa were investigated along the 40 ns MD trajectories. The occupancies (> 40%) of each binding interaction were displayed in **Figure 2**. The result indicated that π-π interaction between the indole ring and Tyr190 showed strong and stable binding. It make a significant contribution to the inhibitory activity of **LX2421** to GPIIb/IIIa (detailed information about the MD simulation can be found in the Supporting Information).

To explore further of this π-π interaction, we designed **LX1**-**LX3** in which a naphthalene ring was used to replace the indole ring in **LX2421** (**Figure 3**). These three compounds vary only in the length of the linker between the naphthyl ring and the piperidine. To our disappointed, none of these compounds inhibit platelet aggregation induced by ADP in human platelet-rich plasma (more precise than the rabbit platelet-rich plasma) at 100 μM (**Table 1**). However surprisingly, **LX4**-**LX6** in which a piperizine ring was used to replace the piperidine ring in **LX1**-**LX3** have much improved activity in inhibiting platelet aggregation, indicating that piperazine is more favorable in this scaffold. Among these three compounds, **LX5** which contains a three CH_2 linker is the most potent one with an IC_{50} value of 0.37 μM, being 60 folds more potent than two CH_2 containing **LX4** and 90 folds more potent than four CH_2 containing **LX6**, thus **LX5** was selected as a new lead for the subsequent study.

Using **LX5** as the lead compound, at first we explored the hydrophobic group on sulfonamide by designing compounds **LX14**-**LX18**. Our results indicated that removing the bromo atom (**LX14**, IC_{50}= 0.18 μM) or replacing it with other electron withdrawn groups, such as fluoro atom (**LX15**, IC_{50}= 0.28 μM) or nitro group (**LX16**, IC_{50}= 0.20 μM) can only slightly influence the antiplatelet activity, but introducing an electron donated methoxy group to the para position of the phenyl ring decreases the

activity by about 8 folds, indicating that the electronic property of the phenyl ring may have influence to the activity. Replacing the phenyl group in **LX14** with a butyl group (**LX18**, IC_{50}= 0.52 μM) decreases the activity by about 3 folds, suggesting phenyl ring is more favorable at this site.

We have also designed a series of compounds by replacing the sulfonamide group with an amide group by designing compounds **LX7**-**LX13**. Our results indicated that amide containing compounds are dramatically less potent than their sulfonamide containing analogues. For example, **LX7** shows an IC_{50} value of 7.9 μM, being more than 40 times less potent than **LX14**, indicating the importance of the sulfonamide structure for the activity.

Our results have indicated that the piperizine group is critical to the antiplatelet activity. Therefore, in order to explore the influence of the basic group, we designed a series of benzamidine containing compounds (**Table 3**), as benzamidine has been frequently used in GPIIb/IIIa antagonists in many published literatures. Both the sulfonamide and the amide containing scaffolds were used in this series. To our delight, at 50 μM several compounds, including **LX24**, **LX25**, **LX26**, **LX30** can reach >99.5% of inhibition, indicating benzamidine can also be used as the base group in our new scaffold. Interestingly, unlike the piperizine containing compounds, sulfonamide containing compounds don't show dramatically more potent activity than the amide containing compounds in this series.

LX14 and **LX25** are two of the most potent inhibitors of platelet aggregation in our two new series of compounds with IC_{50} values of 0.18 μM and 0.84 μM, respectively. Therefore these two compounds are selected for further evaluation. It is noticeable that **LX14** is almost as potent as **Tirofiban**.

2.2 The biologic assay and docking study

Besides ADP, platelet aggregation can also be activated by other inducers. Therefore, **LX14** and **LX25** have also been evaluated for their antiplatelet aggregation activity induced by collagen, collagen and thrombin together with ADP. As shown in **Figure 4** and **Table 4**, **LX14** and **LX25** can significantly inhibit platelet aggregation induced by ADP (20 μM), collagen (1 μg/ml), thrombin (0.26 U/ml) and U46619 (2 μM) with the IC_{50} values of 0.18, 1.32, 0.53, 1.01 μM and 0.84, 27.7, 22.9, 23.6 μM respectively, suggesting that our compounds **LX14** and **LX25** can block the common pathway of platelet aggregation by inhibiting the GPIIb/IIIa receptor. Interestingly, our compounds are more potent in inhibiting platelet aggregation induced by ADP than those induced by other three inducers.

LX14 and **LX25** have been evaluated for their binding affinity to GPIIb/IIIa receptor in the

fibrinogen/GPIIb/IIIa enzyme-linked immunosorbent assay (ELISA) in comparison with **Tirofiban** (**Figure 5)**. Compounds **LX14** and **LX25** can potently block the binding of GPIIb/IIIa to the fibrinogen in a concentration-dependent manner with the IC_{50} values of 0.08 and 1.33 μM respectively, with **LX14** being only two-fold less potent than **Tirofiban**, consistent to its activity in the inhibition of the antiplatelet aggregation. Thus, **LX14** represents a promising GPIIb/IIIa receptor antagonist against platelet aggregation.

In order to probe the binding modes of compounds **LX14** and **LX25** with GPIIb/IIIa, we performed molecular docking study using CDOCKER in Discovery studio 3.0 in comparison with **Tirofiban** (**Figure 6**). The result indicated that **LX14** binds to the same pocket as Tirofiban. **LX14** has hydrogen bond interactions with Ser123 and Asn215 residues and salt bridge interaction with the MIDAS Mg^{2+} ion of GPIIIa as **Tirofiban**. Also similar to **Tirofiban**, the sulfonamido group in **LX14** forms hydrogen bonds with Arg214 and Asn215 residues, and the 4-piperizyl group formed a slat bridge with Asp224 residue, while the naphthalene of **LX14** exhibits π-π interaction with the phenyl ring of Tyr190. The interaction between **LX25** and GPIIb/IIIa is similar to that between **LX14** and GPIIb/IIIa, however, the sulfonamido group in **LX25** doesn't have hydrogen bond interactions with Arg214 and Asn215 residues due to the spatial shift of the amide bond, maybe this is the reason for its less potent binding affinity to GPIIb/IIIa than **LX14.**

The risk of bleeding is one critical limitation for GPIIb/IIIa inhibitors in the preventing formation of thrombus. Therefore, **LX14** has been evaluated for the bleeding times *in vivo* in comparison with **Tirofiban**. As shown in **Figure 7**, treatment with 3 mg/kg, 15 mg/kg and 30 mg/kg of **LX14**, the bleeding times are approximately 6.72±1.23, 8.63±2.14 and 9.28±3.21 min (n= 6) respectively. While only with 1 mg/kg of **Tirofiban**, the bleeding times are 16.8±2.33 min (n= 6). This result indicated that **LX14** has much lower bleeding risk than **Tirofiban**, representing a safer GPIIb/IIIa inhibitor against platelet aggregation.

LX14 has also been evaluated for its *in vivo* antithrombotic activity in comparison with **Tirofiban** in rat arterio-venous shunt model (**Figure 8)**. Our results indicated that **LX14** significantly decreases the thrombus weight in a dose-dependent manner. At 10 mg/kg, it reduces the experimental thrombosis by 40.0±5.8% (n= 6), as effective as **Tirofiban** at 1 mg/kg (37.1±4.7%), further confirming that it is a promising antiplatelet agent.

2.3 Chemistry

Compound **1** was prepared by a described method reported by A. V. Marco, R. Frank *et al* [24].

Reactions of compound **1** with various acyl chloride or sulfonyl chloride afforded **2-15** which were further hydrolyzed with LiOH to yield intermediates **16-29** as shown in scheme **1**. Then, **16-29** were reacted with 4-piperidyl contained intermediates to provide **LX1-LX3** with Boc cleavage. Methylation of **16-29** with $SOCl_2$/MeOH yielded our critical intermediates **30-43**. Compounds **43-57** were further obtained by treatment with the corresponding dibromide, which were reacted with Boc-paperazine to give **58-72**. Finally, **LX4-LX18** were achieved by hydrolyzation of methyl ester and deprotection of Boc. Additionally, **30-43** were refluxed with 4-cyano benzylbromide in dry acetone/K_2CO_3 to give **73-84** which were reacted with HCl/MeOH and NH_3/MeOH by Pinner reaction and hydrolyzed to afford **LX19-LX30**.

3. Conclusion

In summary, we identified compound **LX5** as a novel lead by structure modification of **LX2421**. The antiplatelet aggregation activity of it was more potent than **LX2421** with the IC_{50} value of 7.9 μM. Further optimization, a novel series of compounds were designed and synthesized by exploring the impact of the basic group and the functional group on the α-amino group on the antiplatelet aggregation activity. Our effort led to the hit of **LX14** and **LX25**, showing remarkably antiplatelet aggregation activity, especially **LX14**, almost equally high potency as **Tirofiban**. Further study, **LX14** and **LX25** could inhibit the platelet aggregation induced by four different agonists, **LX14** displayed comparable ability as **Tirofiban** in inhibiting the GPIIb/IIIa receptor (IC_{50}= 0.08 μM). At last, **LX14** was selected to perform *in vivo* biologic evaluation in comparison with **Tirofiban**. The lower bleeding time and significant antithrombotic activity were observed. Above all, **LX14** could be a safer and promising antiplatelet aggregation agent for further study.

4. Experimental procedures

4.1 Chemistry

All reagents were from commercial sources. With tetramethylsilane (TMS) as internal standard, the ^{1}H-NMR and ^{13}C-NMR were recorded on Bruker AV-300 apparatus by using deuterated solvents. HR-MS was collected on Agilent technologies 6520 Accurate-Mass Q-TOF LC/MS instruments. Every targeted compound was purified via silica gel (60Å, 70-230 mesh) column chromatography. Melting points were measured by XT-4 melting point apparatus. The purity (≥95%) of final compounds is verified by the HPLC study performed on Agilent C18 (4.6 mm×150 mm, 3.5 μm) column using a mixture of solvent methanol/water at the flow rate of 0.5 mL/min and peak detection at 254 nm under UV.

(±)-2-Amino-3-(6-hydroxy-2-naphthyl)propanoic acid hydrobromide (2·HBr) **1** was synthesized by a known method established within the literature.

*4.1.1 Typical procedure for the preparation of **2~15***

To the mixture of (±)-2-Amino-3-(6-hydroxy-2-naphthyl)propanoic acid hydrobromide (2·HBr) **1** (4.30 mmol) in acetone (20 mL) and water (10 mL), K_2CO_3 (13.0 mmol) was added, followed by stirring at room temperature for 1 h, then substituted acyl chloride (5.60 mmol) was dropped slowly at 0℃, and the mixture was kept under stirring for 10 h at 65℃. After the reaction was completed, monitored by TLC, the solvent was removed under reduced pressure, and the resulting residue was dissolved in H_2O (10 mL), acidified to pH 2-3 with 1 M HCl, then extracted with AcOEt (3×15mL). The combined organic layers were dried over Na_2SO_4 and concentrated under reduced pressure. The crude residue was purified by flash column chromatography (petroleum ether/AcOEt 1:1) to give the corresponding product.

*4.1.2 Typical procedure for the preparation of **16~29***

To the solution of the intermediate **2~15** (3.80 mmol) in MeOH/Acetone/H_2O (30 mL, v:v:v=1:1:1), LiOH•H_2O (11.0 mmol) was added. The reaction mixture was stirred for 8 h at 50℃, and TLC analysis indicated that the reaction was completed. The solvent was removed under reduced pressure, and the resulting slurry was taken up in H_2O, acidified to pH 2-3 with 1 M HCl. The precipitate was filtered and dried to afford the corresponding compound**.**

*4.1.3 Typical procedure for the preparation of **LX1~LX3***

1-Boc-4-(methylsulfonyl)oxy)propyl) piperidine or 1-Boc-4-(2-((methylsulfonyl)oxy)propyl) piperidine or 1-Boc-4-(2-((methylsulfonyl)oxy)propyl)piperidine or 1-Boc-4-(3-((methylsulfonyl)oxy)propyl) piperidine or 1-Boc-4-(4-((methylsulfonyl)oxy)butyl) piperidine (2.20 mmol) was added to a solution of the amino-substituted derivatives of (±)-2-Amino-3-(6-hydroxy-2-naphthyl)propanoic acid hydrobromide (2·HBr) (**16**~**29**,1.70 mmol) in 15 mL of dry DMF, then dry K_2CO_3 power (5.10 mmol) was added. The mixture was stirred at 80 ℃ for 12 h under N_2, and TLC analysis indicated the reaction was complete. The mixture was filtered, and the filtrate was concentrated in *vacuo*. The crude residue was purified by flash column chromatography and eluted with 2:1 petroleum ether/AcOEt to give the corresponding intermediate. The intermediate was dissolved in 5 ml AcOEt. Pass the dry HCl gas at 0℃ through the system and the solution was stirred and monitored by TLC. After completion, the solvent was removed in vacuo and the residue was

dissolved in methanol. The solution was concentrated in *vacuo* to give the corresponding compound **LX1~LX3**.

*4.1.3.1 (±)-2-((4-bromophenyl)sulfonamido)-3-(6-(piperidin-4-ylmethoxy)naphthalen-2-yl) propanoic acid·HCl（**LX1**）*

It was obtained as a light yellow solid in 35% yield. m.p. 134-136℃; HRMS (ESI): m/z, calculated for $C_{25}H_{27}BrN_2O_5S$, 547.0902 $(M+H)^+$, found 547.0913; ^{1}H-NMR (300MHz, DMSO-d_6): δ 9.79 (br, 1H, HCl), 9.01 (s, 1H, *piperidyl*-NH), 8.73 (d, 1H, J= 8.7 Hz, -SO_2-NH-CH-), 7.63~7.06 (m, 10H, Ar-H), 4.11~4.01 (m, 1H, -CH_2-CH-NH-), 3.67 (t, 2H, J= 6.2 Hz, -CH_2-O-), 3.13~2.67 (m, 6H, *piperidyl*-CH_2-N-CH_2- and -CH_2-CH_2-NH-), 1.91~1.15 (m, 5H, *Piperidine*-H); ^{13}C-NMR (75MHz, DMSO-d_6): δ 170.7, 155.1, 139.8, 133.4, 131.7, 130.0, 128.7, 128.0, 127.4, 126.0, 125.9, 118.7, 108.4, 73.1, 67.7, 57.4, 42.2, 37.7, 36.4, 32.8, 32.2, 30.7, 25.7, 24.5 ppm.

*4.1.3.2 (±)-2-((4-bromophenyl)sulfonamido)-3-(6-(2-(piperidin-4-yl)ethoxy)naphthalen-2-yl)propanoic acid·HCl（**LX2**）*

It was obtained as a light yellow solid in 40% yield. m.p. 152-154℃; HRMS (ESI): m/z, calculated for $C_{26}H_{29}BrN_2O_5S$, 561.1059 $(M+H)^+$, found 561.1046; ^{1}H-NMR (300MHz, DMSO-d_6): δ 9.01~8.72 (br, 2H, *piperidyl*-NH and HCl), 8.70 (d, 1H, J= 8.8 Hz, -SO_2-NH-), 7.60~7.04 (m, 10H, Ar-H), 4.01~3.98 (m, 1H, -CH_2-CH-NH-), 3.79~3.77 (m, 2H, -CH_2-O-), 3.15~2.64 (m, 6H, *piperidyl*-CH_2-N-CH_2- and -CH_2-CH_2-NH-), 1.59~1.10 (m, 7H, *Piperidine* and -CH_2-CH_2-O-); ^{13}C-NMR (75MHz, DMSO-d_6): δ 170.7, 155.1, 147.0, 139.9, 133.4, 131.7, 130.0, 128.7, 128.1, 127.4, 125.9, 124.2, 123.1, 122.6, 118.7, 108.4, 62.0, 61.3, 43.0, 42.7, 34.1, 33.6, 31.1, 30.3, 29.3, 28.6 ppm.

*4.1.3.3(±)-2-((4-bromophenyl)sulfonamido)-3-(6-(3-(piperidin-4-yl)propoxy)naphthalen-2-yl)propanoic acid·HCl（**LX3**）*

It was obtained as a light yellow solid in 43% yield. m.p. 146-148℃; HRMS (ESI): m/z, calculated for $C_{27}H_{31}BrN_2O_5S$, 575.1215 $(M+H)^+$, found 575.1215; ^{1}H-NMR (300MHz, DMSO-d_6): δ 9.00~8.69 (s, 1H, *piperidyl*-NH), 8.69 (d, 1H, J= 8.9 Hz, -SO_2-NH-), 8.67~8.45 (br, 1H, HCl), 7.59~7.01 (m, 10H, Ar-H), 4.00 (m, 1H, -CH_2-CH-NH-), 3.98~3.68 (t, 2H, J= 5.8 Hz, -CH_2-O-), 3.17~2.69 (m, 6H, *piperidyl*-CH_2-N-CH_2- and -CH_2-CH_2-NH-), 1.55~0.91 (m, 9H, *Piperidine* and -CH_2-CH_2-CH_2-O-); ^{13}C-NMR (75MHz, DMSO-d_6): δ 170.7, 155.2, 139.9, 133.4, 131.7, 129.9, 128.7, 128.1, 127.4, 125.9, 118.7, 108.4, 64.5, 57.4, 42.9, 40.2, 38.5, 37.8, 32.4, 31.7, 31.3, 31.0, 29.7, 28.9, 28.0, 24.6 ppm.

*4.1.4 Typical procedure for the preparation of **30~43***

To the stirred solution of the intermediate **16**~**29** (49.00 mmol) in methanol (160 mL) at 0℃, sulfoxide chloride (98.00 mmol) was added dropwise, and stirred at 50℃ overnight. After the reaction, monitored by TLC, was complete, the mixture was concentrated *in vacuo*. The corresponding methyl intermediate was obtained by column chromatography.

*4.1.5 Typical procedure for the preparation of **43~57***

To a solution of intermediate **30~43** (22.03 mmol) in acetonitrile (70 mL), 1,2-dibromoethane or 1,3-dibromopropane or 1,4-dibromobutane (44.06 mmol), K_2CO_3 (66.09 mmol) were added. The mixture was stirred at 60℃ for 48 h. The product was filtered, and the filtrate was concentrated in *vacuo*. The crude residue was purified by flash column chromatography and eluted with 5:1 petroleum ether/AcOEt to give the corresponding product.

*4.1.6 Typical procedure for the preparation of **58~72***

To the solution of the intermediate **43~57** in acetonitrile (40 mL), 1-Boc-piperazine (20.40 mmol) and K_2CO_3 (20.40 mmol) were added. The mixture was stirred at 60℃ for 48 h. The reaction was filtered, and the filtrate was concentrated in *vacuo*. The crude residue was purified by flash column chromatography and eluted with 8:1 petroleum ether/AcOEt to give the corresponding product.

*4.1.7 Typical procedure for the preparation of **LX4**~**LX18***

To the solution of the intermediate **58~72** (2.30 mmol) in MeOH/THF/H_2O (15 mL, v:v:v=1:1:1), LiOH•H_2O (6.90 mmol) was added. The reaction mixture was stirred at room temperature for 2 h, and TLC analysis indicated that the reaction was completed. The solvent was removed under reduced pressure, and the resulting slurry was taken up in H_2O, acidified to pH 2-3 with 1 M HCl. The precipitate was filtered and dried to afford the corresponding compound with Boc-piperazine. Then the intermediates (1.50 mmol) were dissolved in 5 ml AcOEt. Pass the dry HCl gas at 0℃ through the system and the solution was stirred and monitored by TLC. After completion, the solvent was removed in vacuo and the residue was dissolved in methanol. The solution was concentrated *in vacuo* to give the corresponding compound.

*4.1.7.1 (±)-2-((4-bromophenyl)sulfonamido)-3-(6-(2-(piperazin-1-yl)ethoxy)naphthalen-2-yl)propanoic acid·HCl（**LX4**）*

It was obtained as a white solid in 41% yield. m.p. 153-155℃; HRMS (ESI): m/z, calculated for $C_{25}H_{28}BrN_3O_5S$, 562.1006 $(M+H)^+$, found 562.1033; ^{1}H-NMR (300MHz, DMSO-d_6): δ 12.3 (s, 1H, -COOH), 9.84 (br, 2H, *piperidyl*-NH and HCl), 8.52~8.49 (d, 1H, J= 9.0 Hz, -SO_2-NH-), 7.71~7.22 (m, 10H, Ar-H), 4.56 (t, 2H, J= 6.0 Hz, -CH_2-O-), 4.01~3.94 (m, 1H, -CH_2-CH-NH-), 3.68~3.50 (m, 10H, *Piperazine* and -CH_2-CH_2-O-), 3.02~2.73 (m, 2H, -CH_2-CH-NH-); ^{13}C-NMR (75MHz, DMSO-d_6): δ 172.2, 155.0, 140.2, 132.8, 132.2, 131.4, 128.9, 128.5, 127.9, 127.8, 127.5, 126.5, 125.6, 118.5, 107.1, 62.4, 57.6, 54.5, 48.4, 37.6, 31.1, 29.8, 21.0 ppm.

4.1.7.2(±)-2-((4-bromophenyl)sulfonamido)-3-(6-(3-(piperazin-1-yl)propoxy)naphthalen-2-yl)propanoic acid·HCl（***LX5***）

It was obtained as a white solid in 45% yield. m.p. 171-173℃; HRMS (ESI): m/z, calculated for $C_{26}H_{30}BrN_3O_5S$, 576.1062 $(M+H)^+$, found 576.1078; ^{1}H-NMR (300MHz, DMSO-d_6): δ 12.3 (s, 1H, -COOH), 9.85 (br, 2H, *piperidyl*-NH and HCl), 8.78 (d, 1H, J= 9.0 Hz, -SO_2-NH-), 7.79~7.10 (m, 10H, Ar-H), 4.20 (t, 2H, J= 5.5 Hz, -CH_2-O-), 4.04~3.98 (m, 1H, -CH_2-CH-NH-), 3.73~3.49 (m, 10H, *Piperazine* and -CH_2-CH_2-CH_2-O-), 3.13~2.77 (m, 2H, -CH_2-CH-NH-), 2.30~2.27 (m, 2H, -CH_2-CH_2-CH_2-O-); ^{13}C-NMR (75MHz, DMSO-d_6): δ 172.2, 155.8, 140.2, 133.0, 131.9, 131.4, 128.8, 128.3, 127.8, 127.5, 126.5, 125.5, 118.5, 106.7, 64.8, 57.6, 53.1, 47.7, 37.6, 31.1, 29.8, 29.2, 23.2 ppm.

4.1.7.3 (±)-2-((4-bromophenyl)sulfonamido)-3-(6-(4-(piperazin-1-yl)butoxy)naphthalen-2-yl)propanoic acid·HCl（***LX6***）

It was obtained as a white solid in 53% yield. m.p. 169-171℃; HRMS (ESI): m/z, calculated for $C_{27}H_{32}BrN_3O_5S$, 590.1319 $(M+H)^+$, found 590.1347; ^{1}H-NMR (300MHz, DMSO-d_6): δ 12.0 (s, 1H, -COOH), 10.1 (br, 2H, *piperidyl*-NH and HCl), 8.80 (d, 1H, J= 9.0 Hz, -SO_2-NH-), 7.66~7.13 (m, 10H, Ar-H), 4.13~4.11 (m, 2H, -CH_2-O-), 3.99~3.97 (m, 1H, -CH_2-CH-NH-), 3.90~3.40 (m, 10H, *Piperazine* and -CH_2-CH_2-CH_2-CH_2-O-), 3.219~3.08 (m, 2H, -CH_2-CH-NH-), 1.91~1.87 (m, 4H, -CH_2-CH_2-CH_2-CH_2-O-); ^{13}C-NMR (75MHz, DMSO-d_6): δ 172.2, 156.1, 140.2, 133.0, 131.8, 131.4, 128.7, 128.2, 127.8, 127.8, 127.4, 126.4, 125.5, 118.6, 106.6, 66.8, 57.6, 55.3, 47.6, 37.6, 25.8, 20.0 ppm.

4.1.7.4 (±)-2-benzamido-3-(6-(3-(piperazin-1-yl)propoxy)naphthalen-2-yl)propanoic acid·HCl（***LX7***）

It was obtained as a white solid in 45% yield. m.p. 171-173℃; HRMS (ESI): m/z, calculated for $C_{27}H_{32}N_3O_4$, 462.2293 $(M+H)^+$, found 462.2230; ^{1}H-NMR (300MHz, DMSO-d_6): δ 9.66 (br, 2H, *piperidyl*-NH and HCl), 8.78 (d, 1H, J= 8.3 Hz, -CO-NH-), 7.79~7.10 (m, 11H, Ar-H), 4.72~4.70 (m,

1H, -CH_2-CH-NH-), 4.15 (t, 2H, J= 6.1 Hz, -CH_2-O-), 3.71~3.30 (m, 10H, *Piperazine* and -CH_2-CH_2-CH_2-O-), 3.29~3.14 (m, 2H, -CH_2-CH-NH-), 2.24~2.22 (m, 2H, -CH_2-CH_2-CH_2-O-); ^{13}C-NMR (75MHz, DMSO-d_6): δ 173.0, 166.5, 155.8, 133.8, 133.6, 133.4, 132.9, 132.8, 131.4, 128.8, 128.4, 128.1, 127.3, 127.2, 127.1, 126.5, 118.5, 106.8, 64.8, 54.4, 53.1, 47.7, 38.6, 36.6, 29.2, 28.9, 14.0 ppm.

4.1.7.5(±)-2-(3-fluorobenzamido)-3-(6-(3-(piperazin-1-yl)propoxy)naphthalen-2-yl)propanoic acid·HCl（***LX8***）

It was obtained as a white solid in 63% yield. m.p. 161-163℃; HRMS (ESI): m/z, calculated for $C_{27}H_{31}FN_3O_4$, 480.2199 $(M+H)^+$, found 480.2125; ^{1}H-NMR (300MHz, DMSO-d_6): δ 11.9 (s, 1H, -COOH), 9.76 (br, 2H, *piperidyl*-NH and HCl), 8.91 (d, 1H, J= 8.3 Hz, -CO-NH-), 7.75~7.10 (m, 10H, Ar-H), 4.72~4.67 (m, 1H, -CH_2-CH-NH-), 4.15 (t, 2H, J= 5.6 Hz, -CH_2-O-), 3.70~3.42 (m, 10H, *Piperazine* and -CH_2-CH_2-CH_2-O-), 3.29~3.14 (m, 2H, -CH_2-CH-NH-), 2.22~1.90 (m, 2H, -CH_2-CH_2-CH_2-O-); ^{13}C-NMR (75MHz, DMSO-d_6): δ 172.8, 165.0 (J= 367 Hz), 163.4, 160.1, 155.8, 136.1, 133.3, 132.9, 132.8, 130.4, 128.8, 128.4, 128.0, 127.1, 126.5, 123.5, 118.5, 118.3, 118.0, 114.2, 106.8, 64.9, 54.4, 53.1, 47.7, 36.2, 23.2, 13.9 ppm.

4.1.7.6(±)-2-(4-fluorobenzamido)-3-(6-(3-(piperazin-1-yl)propoxy)naphthalen-2-yl)propanoic acid·HCl（***LX9***）

It was obtained as a white solid in 65% yield. m.p. 177-179℃; HRMS (ESI): m/z, calculated for $C_{27}H_{31}FN_3O_4$, 480.2199 $(M+H)^+$, found 480.2134; ^{1}H-NMR (300MHz, DMSO-d_6): δ 11.7 (s, 1H, -COOH), 9.56 (br, 2H, *piperidyl*-NH and HCl), 8.83 (d, 1H, J= 8.0 Hz, -CO-NH-), 7.88~7.10 (m, 10H, Ar-H), 4.69 (m, 1H, -CH_2-CH-NH-), 4.16 (t, 2H, J= 5.9 Hz, -CH_2-O-), 3.81~3.30 (m, 10H, *Piperazine* and -CH_2-CH_2-CH_2-O-), 3.21~3.13 (m, 2H, -CH_2-CH-NH-), 2.21~2.20 (m, 2H, -CH_2-CH_2-CH_2-O-); ^{13}C-NMR (75MHz, DMSO-d_6): δ 173.1, 165.5 (J= 247 Hz), 165.2, 162.2, 155.7, 133.4, 132.8, 130.2, 130.0, 129.8, 128.9, 128.4, 128.1, 127.1, 126.5, 118.5, 115.3, 115.0, 106.6, 64.8, 54.3, 53.1, 47.8, 36.2 ppm.

4.1.7.7(±)-2-(3,5-dichlorobenzamido)-3-(6-(3-(piperazin-1-yl)propoxy)naphthalen-2-yl)propanoic acid·HCl（***LX10***）

It was obtained as a light yellow solid in 53% yield. m.p. 149-151℃; HRMS (ESI): m/z, calculated for $C_{27}H_{30}Cl_2N_3O_4$, 530.1413 $(M+H)^+$, found 530.1433; ^{1}H-NMR (300MHz, DMSO-d_6): δ 11.8 (s, 1H, -COOH), 9.63 (br, 2H, *piperidyl*-NH and HCl), 9.04 (d, 1H, J= 8.0 Hz, -CO-NH-), 7.76~7.09 (m, 9H,

Ar-H), 4.65 (m, 1H, -CH_2-CH-NH-), 4.13 (t, 2H, J= 5.8 Hz, -CH_2-O-), 3.80~3.30 (m, 10H, *Piperazine* and -CH_2-CH_2-CH_2-O-), 3.25~3.09 (m, 2H, -CH_2-CH-NH-), 2.22~2.20 (m, 2H, -CH_2-CH_2-CH_2-O-); ^{13}C-NMR (75MHz, DMSO-d_6): δ 172.7, 163.5, 155.8, 136.8, 134.2, 133.1, 132.9, 130.8, 128.8, 128.4, 128.0, 127.2, 126.5, 126.1, 118.6, 106.6, 64.8, 54.4, 53.1, 47.8, 38.6, 36.2, 23.2 ppm.

4.1.7.8 (±)-2-(4-nitrobenzamido)-3-(6-(3-(piperazin-1-yl)propoxy)naphthalen-2-yl)propanoic acid·HCl（***LX11***）

It was obtained as a yellow solid in 60% yield. m.p. 144-146℃; HRMS (ESI): m/z, calculated for $C_{27}H_{31}N_4O_6$, 507.2044 $(M+H)^+$, found 507.2060; ^{1}H-NMR (300MHz, DMSO-d_6): δ 10.0 (br, 2H, *piperidyl*-NH and HCl), 9.28 (d, 1H, J= 7.7 Hz, -CO-NH-), 8.18~6.98 (m, 10H, Ar-H), 4.62 (m, 1H, -CH_2-CH-NH-), 3.97 (t, 2H, J= 6.0 Hz, -CH_2-O-), 3.43~3.30 (m, 10H, *Piperazine* and -CH_2-CH_2-CH_2-O-), 3.21~3.14 (m, 2H, -CH_2-CH-NH-), 2.15~2.11 (m, 2H, -CH_2-CH_2-CH_2-O-); ^{13}C-NMR (75MHz, DMSO-d_6): δ 171.5, 162.5, 157.1, 153.2, 138.5, 134.1, 133.5, 130.6, 127.4, 127.0, 126.8, 126.6, 126.3, 124.5, 123.5, 123.0, 122.4, 122.6, 114.1, 106.2, 106.1, 102.4, 55.2, 52.1, 44.2, 41.3 ppm.

4.1.7.9(±)-2-(4-methoxybenzamido)-3-(6-(3-(piperazin-1-yl)propoxy)naphthalen-2-yl)propanoic acid·HCl（***LX12***）

It was obtained as a light yellow solid in 53% yield. m.p. 166-168℃; HRMS (ESI): m/z, calculated for $C_{28}H_{34}N_3O_5$, 492.2398 $(M+H)^+$, found 492.2312; ^{1}H-NMR (300MHz, DMSO-d_6): δ 9.55 (s, 2H, *piperidyl*-NH and HCl), 8.62 (d, 1H, J= 8.3 Hz, -CO-NH-), 7.79~6.94 (m, 10H, Ar-H), 4.67~4.64 (m, 1H, -CH_2-CH-NH-), 4.15 (t, 2H, J= 5.8 Hz, -CH_2-O-), 3.74 (s, 3H, CH_3-O-), 3.44~3.31 (m, 10H, *Piperazine* and -CH_2-CH_2-CH_2-O-), 3.28~3.13 (m, 2H, -CH_2-CH-NH-), 2.24~2.21 (m, 2H, -CH_2-CH_2-CH_2-O-); ^{13}C-NMR (75MHz, DMSO-d_6): δ 173.3, 165.7, 161.6, 155.7, 133.5, 132.8, 129.1, 128.9, 128.4, 128.1, 127.1, 126.4, 126.0, 118.5, 113.3, 106.6, 64.7, 59.7, 55.2, 54.2, 53.0, 47.8, 36.2, 31.3, 30.5, 29.6, 23.1, 14.0 ppm.

4.1.7.10 (±)-2-butyramido-3-(6-(3-(piperazin-1-yl)propoxy)naphthalen-2-yl)propanoic acid·HCl（***LX13***）

It was obtained as a light yellow solid in 33% yield. m.p. 155-157℃; HRMS (ESI): m/z, calculated for $C_{24}H_{34}N_3O_4$, 428.2549 $(M+H)^+$, found 428.2551; ^{1}H-NMR (300MHz, DMSO-d_6): δ 11.9 (s, 1H, -COOH), 9.76 (br, 2H, *piperidyl*-NH and HCl), 8.15 (d, 1H, J= 8.1 Hz, -CO-NH-), 7.72~7.09 (m, 6H, Ar-H), 4.47 (m, 1H, -CH_2-CH-NH-), 4.15 (t, 2H, J= 5.8 Hz, -CH_2-O-), 3.70~3.42 (m, 10H, *Piperazine* and -CH_2-CH_2-CH_2-O-), 3.17~2.92 (m, 2H, -CH_2-CH-NH-), 2.24~2.22 (m, 2H, -CH_2-CH_2-CH_2-O-),

2.00~1.87 (m, 2H, -$\underline{CH_2}$-CH_2-CH_3), 1.42~1.29 (m, 2H, -CH_2-$\underline{CH_2}$-CH_3), 0.65 (t, 3H, J= 7.1 Hz, -CH_2-CH_2-$\underline{CH_3}$); ^{13}C-NMR (75MHz, DMSO-d_6): δ 173.2, 171.9, 155.7, 133.0, 132.8, 128.9, 128.4, 128.0, 127.2, 126.4, 118.5, 106.6, 64.8, 53.3, 53.0, 47.7, 36.9, 36.7, 30.8, 23.1, 18.5, 13.5, 13.3 ppm.

4.1.7.11(±)-2-(phenylsulfonamido)-3-(6-(3-(piperazin-1-yl)propoxy)naphthalen-2-yl)propanoic acid·HCl（***LX14***）

It was obtained as a light yellow solid in 43% yield. m.p. 174-176℃; HRMS (ESI): m/z, calculated for $C_{26}H_{32}N_3O_5S$, 498.2063 $(M+H)^+$, found 498.2046; ^{1}H-NMR (300MHz, DMSO-d_6): δ 12.1 (s, 1H, -COOH), 9.89 (br, 2H, HCl and *piperazine*-$\underline{NH}$), 8.32 (d, 1H, J= 9.06 Hz, -SO_2-$\underline{NH}$-), 7.67~7.09 (m, 11H, Ar-H), 4.16 (t, 2H, J= 5.8 Hz, -$\underline{CH_2}$-O-), 3.95~3.91 (m, 1H, -CH_2-$\underline{CH}$-NH-), 3.71~3.07 (m, 10H, *Piperazine* and -$\underline{CH_2}$-CH_2-CH_2-O-), 3.07~2.76 (m, 2H, -$\underline{CH_2}$-CH-NH-), 2.46~2.22 (m, 2H, -CH_2-$\underline{CH_2}$-CH_2-O-); ^{13}C-NMR (75MHz, DMSO-d_6): δ 172.2, 155.8, 140.9, 133.0, 131.9, 131.8, 128.9, 128.7, 128.5, 128.3, 128.1, 127.9, 127.4, 127.2, 126.5, 126.1, 126.0, 118.4, 106.6, 64.8, 57.4, 53.0, 47.7, 37.7, 23.2 ppm.

4.1.7.12(±)-2-((4-fluorophenyl)sulfonamido)-3-(6-(3-(piperazin-1-yl)propoxy)naphthalen-2-yl)propanoic acid·HCl（***LX15***）

It was obtained as a light yellow solid in 38% yield. m.p. 159-161℃; HRMS (ESI): m/z, calculated for $C_{26}H_{31}FN_3O_5S$, 516.1968 $(M+H)^+$, found 516.1953; ^{1}H-NMR (300MHz, DMSO-d_6): δ 11.9 (s, 1H, -COOH), 9.70 (br, 2H, HCl and *piperazine*-$\underline{NH}$), 8.42 (d, 1H, J= 9.1 Hz, -SO_2-$\underline{NH}$-), 7.67~6.97 (m, 10H, Ar-H), 4.15 (t, 2H, J= 5.8 Hz, -$\underline{CH_2}$-O-), 3.99~3.90 (m, 1H, -CH_2-$\underline{CH}$-NH-), 3.72~3.30 (m, 10H, *Piperazine* and -$\underline{CH_2}$-CH_2-CH_2-O-), 3.10~3.04 (m, 2H, -$\underline{CH_2}$-CH-NH-), 2.30~2.25 (m, 2H, -CH_2-$\underline{CH_2}$-CH_2-O-); ^{13}C-NMR (75MHz, DMSO-d_6): δ 173.5, 165.3 (J= 150 Hz), 162.2, 163.3, 151.1, 131.7, 128.7, 128.6, 128.4, 128.1, 127.4, 127.0, 126.4, 125.1, 124.5, 119.1, 111.3, 112.0, 110.8, 109.6, 102.0, 67.1, 55.8, 54.7, 48.0 ppm.

4.1.7.13(±)-2-((4-methoxyphenyl)sulfonamido)-3-(6-(3-(piperazin-1-yl)propoxy)naphthalen-2-yl)propanoic acid·HCl（***LX17***）

It was obtained as a light yellow solid in 40% yield. m.p. 158-160℃; HRMS (ESI): m/z, calculated for $C_{27}H_{34}N_3O_6S$, 528.2168 $(M+H)^+$, found 528.2151; ^{1}H-NMR (300MHz, DMSO-d_6): δ9.90 (br, 2H, HCl and *piperazine*-$\underline{NH}$), 8.14 (d, 1H, J= 8.9 Hz, -SO_2-$\underline{NH}$-), 7.64~6.66 (m, 10H, Ar-H), 4.19~4.11 (m, 2H, -$\underline{CH_2}$-O-), 3.87~3.85 (m, 1H, -CH_2-$\underline{CH}$-NH-), 3.66~3.30 (m, 13H, *Piperazine* and -$\underline{CH_2}$-CH_2-CH_2-O- and $\underline{CH_3}$-O-), 3.00~2.46 (m, 2H, -$\underline{CH_2}$-CH-NH-), 2.25~2.22 (m, 2H, -CH_2-$\underline{CH_2}$-CH_2-O-); ^{13}C-NMR

(75MHz, DMSO-d_6): δ 171.1, 170.8, 155.3, 152.1, 151.8, 151.3, 150.1, 136.1, 135.2, 134.1, 133.5, 131.8, 127.1, 126.8, 126.3, 126.1 125.3, 122.2, 121.0, 120.5, 67.8, 66.5, 45.2, 43.5 ppm.

4.1.7.14(±)-2-(butylsulfonamido)-3-(6-(3-(piperazin-1-yl)propoxy)naphthalen-2-yl)propanoic acid·HCl (***LX18***)

It was obtained as a light yellow solid in 33% yield. m.p. 167-169℃; HRMS (ESI): m/z, calculated for $C_{24}H_{36}N_3O_5S$, 478.2376 $(M+H)^+$, found 478.2361; ^{1}H-NMR (300MHz, DMSO-d_6): δ 11.9 (s, 1H, -COOH), 9.70 (s, 2H, *piperidyl*-NH and HCl), 7.79~7.14 (m, 6H, Ar-H), 4.20 (m, 1H, -CH_2-CH-NH-), 4.11 (m, 2H, -CH_2-O-), 3.45~3.37 (m, 10H, *Piperazine* and -CH_2-CH_2-CH_2-O-), 3.26~2.89 (m, 2H, -CH_2-CH-NH-), 2.26~2.23 (m, 2H, -CH_2-CH_2-CH_2-O-), 1.27~1.24 (m, 2H, -CH_2-CH_2-CH_2-CH_3), 1.18~1.15 (m, 2H, -CH_2-CH_2-CH_2-CH_3), 0.96~0.87 (m, 2H, -CH_2-CH_2-CH_2-CH_3), 0.55 (t, 3H, J= 7.5Hz, -CH_2-CH_2-CH_2-CH_3); ^{13}C-NMR (75MHz, DMSO-d_6): δ 173.1, 155.9, 133.0, 132.6, 129.2, 128.9, 128.3, 128.1, 127.7, 126.5, 118.6, 106.7, 64.9, 57.5, 53.1, 52.2, 47.8, 38.5, 37.7, 24.8, 23.4, 20.5, 13.1 ppm.

*4.1.8 Typical procedure for the preparation of **73~84***

To the solution of the intermediate **30~43** (10.20 mmol) in acetonitrile (40 mL), 4-cyanobenzyl bromide (15.30 mmol) and K_2CO_3 (20.40 mmol) were added. The mixture was refluxed overnight. The reaction was filtered, and the filtrate was concentrated in *vacuo*. The crude residue was purified by flash column chromatography and eluted with 1:1 petroleum ether/AcOEt to give the corresponding product.

*4.1.9 Typical procedure for the preparation of **LX19~LX30***

The intermediate **73~84** (2.30 mmol) was dissolved in dry MeOH (3 mL), Pass the dry HCl gas at 0℃ through the system and the solution was stirred for 8h and monitored by TLC. After completion, the solvent was removed in vacuo and the residue was dissolved in dry methanol (3ml) again. Pass the dry NH_3 gas through the system at room temperature and the solution was stirred for 6h and monitored by TLC. After completion, the solvent was removed in vacuo and the residue was dissolved in AcOEt. Then, the crude residue was purified by flash column chromatography and eluted with 10:1 AcOEt /MeOH to give the corresponding intermediate.

To the solution of the intermediate (1.30 mmol) in MeOH/THF/H_2O (3 mL, v:v:v=1:1:1), LiOH•H_2O (2.60 mmol) was added. The reaction mixture was stirred at room temperature overnight.

After the reaction, monitored by TLC, was completed, the solvent was removed under reduced pressure, and the mixture was diluted in H_2O, acidified to pH 2-3 with 1 M HCl. The precipitate was filtered and dried to afford the corresponding compound.

4.1.9.1(±)-2-benzamido-3-(6-((4-carbamimidoylbenzyl)oxy)naphthalen-2-yl)propanoic acid·HCl（***LX19***）

It was obtained as a grey solid in 45% yield. m.p. 181-184℃; HRMS (ESI): m/z, calculated for $C_{28}H_{25}N_3O_4$, 468.2012 $(M+H)^+$, found 468.2006; ^{1}H-NMR (300MHz, DMSO-d_6): δ9.65 (br, 1H, HCl), 8.56 (d, 1H, J= 8.3 Hz, -CO-NH-), 7.79~7.00 (m, 18H, Ar-H and NH =C-NH_2), 5.51 (m, 1H, -CH_2-CH-NH-), 4.73~4.59 (m, 2H, -CH_2-O-), 3.25~3.00 (m, 2H, -CH_2-CH-NH-); ^{13}C-NMR (75MHz, DMSO-d_6): δ 173.3, 166.0, 165.4, 162.2, 162.0, 154.8, 148.8, 134.0, 133.1, 132.6, 131.1, 128.7, 128.1, 128.0, 127.9, 127.8, 127.5, 127.4, 127.3, 127.2, 127.1, 126.4, 125.6, 118.5, 108.4, 62.1, 54.9, 37.2 ppm.

4.1.9.2(±)-2-(3-fluorobenzamido)-3-(6-((4-carbamimidoylbenzyl)oxy)naphthalen-2-yl)propanoic acid·HCl（***LX20***）

It was obtained as a light yellow solid in 41% yield. m.p. 182-185℃; HRMS (ESI): m/z, calculated for $C_{28}H_{24}FN_3O_4$, 486.1954 $(M+H)^+$, found 486.1940; ^{1}H-NMR (300MHz, DMSO-d_6): δ9.70~9.23 (m, 3H, NH=C-NH_2), 8.72 (d, 1H, J= 6.1 Hz, -CO-NH-), 7.87~7.16 (m, 14H, Ar-H), 5.31~5.21 (m, 2H, -CH_2-O-), 4.63 (m, 1H, -CH_2-CH-NH-), 3.30~30.1 (m, 2H, -CH_2-CH-NH-); ^{13}C-NMR (75MHz, DMSO-d_6): δ 173.4, 167.5 (J= 210 Hz), 165.6, 164.7, 155.7, 143.0, 140.1, 136.5, 133.9, 133.7, 132.7, 130.4, 130.2, 129.0, 128.5, 128.0, 127.6, 126.4, 123.5, 118.6, 118.2, 117.9, 114.3, 113.8, 107.3, 68.2, 55.0, 37.2 ppm.

4.1.9.3(±)-2-(4-fluorobenzamido)-3-(6-((4-carbamimidoylbenzyl)oxy)naphthalen-2-yl)propanoic acid·HCl（***LX21***）

It was obtained as a red solid in 48% yield. m.p. 183-184℃; HRMS (ESI): m/z, calculated for $C_{28}H_{24}FN_3O_4$, 486.1966 $(M+H)^+$, found 486.1963; ^{1}H-NMR (300MHz, DMSO-d_6): δ9.43~9.34 (m, 3H, NH=C-NH_2), 8.85~8.73 (d, 1H, J= 8.5 Hz, -CO-NH-), 7.89~7.16 (m, 14H, Ar-H), 5.30~5.21(m, 2H, -CH_2-O-), 4.68~4.55 (m, 1H, -CH_2-CH-NH-), 3.29~3.13 (m, 2H, -CH_2-CH-NH-); ^{13}C-NMR (75MHz, DMSO-d_6): δ 173.3, 167.6 (J= 405 Hz), 165.2, 162.2, 155.4, 143.1, 134.0, 133.6, 132.7, 130.5, 129.9, 129.4, 129.0, 128.5, 128.3, 127.6, 127.2, 126.5, 118.3, 115.2, 114.9, 107.3, 68.6, 68.2, 55.1, 54.4, 37.2, 36.3 ppm.

4.1.9.4(±)-2-(4-nitrobenzamido)-3-(6-((4-carbamimidoylbenzyl)oxy)naphthalen-2-yl)propanoic

acid·HCl（***LX22***）

It was obtained as a light yellow solid in 35% yield. m.p. 178-179℃; HRMS (ESI): m/z, calculated for $C_{28}H_{24}N_4O_6$, 513.1789 $(M+H)^+$, found 513.1797; ^{1}H-NMR (300MHz, DMSO-d_6): δ 10.2~9.22 (NH=C-NH_2), 8.86 (d, 1H, J= 7.4 Hz, -CO-NH-), 8.26~7.16 (m, 17H, Ar-H), 5.30~5.21 (m, 2H, -CH_2-O-), 4.61 (m, 1H, -CH_2-CH-NH-), 3.28~3.10 (m, 2H, -CH_2-CH-NH-); ^{13}C-NMR (75MHz, DMSO-d_6): δ 174.1, 172.9, 167.5, 165.6, 164.4, 155.6, 148.9, 148.8, 142.9, 140.1, 134.2, 133.8, 133.6, 132.7, 129.0, 128.8, 128.3, 128.1, 127.7, 127.1, 126.3, 123.3, 118.5, 107.2, 68.6, 55.9, 55.4, 55.2 ppm.

4.1.9.5(±)-2-(4-methoxybenzamido)-3-(6-((4-carbamimidoylbenzyl)oxy)naphthalen-2-yl)propanoic acid·HCl（***LX23***）

It was obtained as a yellow solid in 46% yield. m.p. 184-187℃; HRMS (ESI): m/z, calculated for $C_{29}H_{27}N_3O_5$, 498.2021 $(M+H)^+$, found 498.2063; ^{1}H-NMR (300MHz, DMSO-d_6): δ7.99~6.87 (m, 17H, Ar-H and NH=C-NH_2), 5.19 (m, 2H, -CH_2-O-), 4.51 (m, 1H, -CH_2-CH-NH-), 3.73 (m, 2H, CH_3-O-), 3.20~3.10 (m, 2H, -CH_2-CH-NH-); ^{13}C-NMR (75MHz, DMSO-d_6): δ 167.6, 165.0, 161.3, 155.4, 140.2, 134.7, 133.6, 132.5, 129.1, 128.8, 128.7, 128.4, 128.2, 127.9, 127.6, 127.4, 127.1, 126.9, 126.0, 118.4, 113.3, 107.0, 68.6, 55.7, 55.2 ppm.

4.1.9.6(±)-2-butyramido-3-(6-((4-carbamimidoylbenzyl)oxy)naphthalen-2-yl)propanoic acid·HCl（***LX24***）

It was obtained as a yellow solid in 40% yield. m.p. 188-190℃; HRMS (ESI): m/z, calculated for $C_{25}H_{27}N_3O_4$, 434.2281 $(M+H)^+$, found 434.2270; ^{1}H-NMR (300MHz, DMSO-d_6): δ 12.6 (s, 1H, -COOH), 9.42~9.24 (m, 3H, NH=C-NH_2), 8.20 (d, 1H, J= 8.1 Hz, -CO-NH-), 7.80~7.04 (m, 10H, Ar-H), 5.35~5.26 (m, 2H, -CH_2-O-), 4.48 (m, 1H, -CH_2-CH-NH-), 3.20~2.92 (m, 2H, -CH_2-CH-NH-), 2.00 (m, 2H, -CH_2-CH_2-CH_3), 1.98~1.34 (m, 2H, -CH_2-CH_2-CH_3), 0.68 (t, 2H, J= 7.1 Hz, -CH_2-CH_2-CH_3); ^{13}C-NMR (75MHz, DMSO-d_6): δ 173.2, 172.0, 167.5, 165.4, 155.7, 155.4, 143.1, 140.1, 133.6, 133.2, 132.8, 129.0, 128.5, 128.2, 128.1, 127.6, 126.4, 118.6, 107.2, 107.1, 68.6, 68.2, 53.3, 18.5, 13.3 ppm.

4.1.9.7(±)-2-(phenylsulfonamido)-3-(6-((4-carbamimidoylbenzyl)oxy)naphthalen-2-yl)propanoic acid·HCl（***LX25***）

It was obtained as a light yellow solid in 48% yield. m.p. 182-185℃; HRMS (ESI): m/z, calculated for $C_{27}H_{25}N_3O_5S$, 504.1633 $(M+H)^+$, found 504.1656; ^{1}H-NMR (300MHz, DMSO-d_6): δ 12.8 (s, 1H,

-COOH), 9.38~9.17 (m, 3H, NH=C-NH_2), 8.34~8.30 (d, 1H, J= 9.2 Hz, -SO_2-NH-), 7.89~7.19 (m, 14H, Ar-H), 5.35 (m, 2H, -CH_2-O-), 3.91~3.89 (m, 1H, -CH_2-CH-NH-), 2.83~2.77 (m, 2H, -CH_2-CH-NH-); ^{13}C-NMR (75MHz, DMSO-d_6): δ 172.2, 165.4, 155.5, 143.2, 140.9, 132.9, 132.4, 132.1, 131.8, 129.1, 128.5, 128.4, 128.3, 128.0, 127.6, 127.5, 127.3, 127.2, 126.5, 126.0, 118.6, 107.2, 68.2, 57.4 ppm.

4.1.9.8(±)-2-((4-methylphenyl)sulfonamido)-3-(6-((4-carbamimidoylbenzyl)oxy)naphthalen-2-yl)propanoic acid·HCl（***LX26***）

It was obtained as a yellow solid in 42% yield. m.p. 177-180℃; HRMS (ESI): m/z, calculated for $C_{28}H_{27}N_3O_5S$, 518.1823 $(M+H)^+$, found 518.1818; ^{1}H-NMR (300MHz, DMSO-d_6): δ 9.71 (br, 1H, HCl), 9.35 (d, 1H, J= 6.1 Hz, -SO_2-NH-), 8.02~6.98 (m, 17H, Ar-H and NH=C-NH_2), 5.37~5.28 (m, 2H, -CH_2-O-), 4.68~4.61 (m, 1H, -CH_2-CH-NH-), 3.10~2.70 (m, 2H, -CH_2-CH-NH-), 2.20 (s, 3H, CH_3-); ^{13}C-NMR (75MHz, DMSO-d_6): δ 172.5, 167.5, 155.4, 143.1, 141.9, 137.9, 132.9, 132.3, 129.4, 128.9, 128.4, 128.3, 128.2, 127.6, 127.4, 127.2, 126.3, 126.0, 118.5, 57.5, 68.4, 58.3, 36.1, 20.9, 20.8 ppm.

4.1.9.9(±)-2-((4-methoxyphenyl)sulfonamido)-3-(6-((4-carbamimidoylbenzyl)oxy)naphthalen-2-yl)propanoic acid·HCl（***LX27***）

It was obtained as a light yellow solid in 33% yield. m.p. 178-181℃; HRMS (ESI): m/z, calculated for $C_{28}H_{27}N_3O_6S$, 534.1728 $(M+H)^+$, found 534.1704; ^{1}H-NMR (300MHz, DMSO-d_6): δ 12.8 (s, 1H, -COOH), 9.45~9.32 (m, 3H, NH=C-NH_2), 9.20 (br, 1H, HCl), 8.17 (d, 1H, J= 8.0 Hz, -SO_2-NH-), 8.19~6.73 (m, 14H, Ar-H), 5.44~5.28 (m, 2H, -CH_2-O-), 4.81~4.36 (m, 1H, -CH_2-CH-NH-), 3.89 (s, 3H, CH_3-O-), 3.11~2.82 (m, 2H, -CH_2-CH-NH-); ^{13}C-NMR (75MHz, DMSO-d_6): δ 172.4, 167.5, 165.4, 161.6, 155.8, 143.1, 140.1, 132.8, 132.2, 129.1, 128.4, 128.3, 128.2, 127.6, 127.4, 126.5, 126.3, 118.3, 113.6, 113.4, 107.1, 107.0, 68.7, 68.2, 57.7, 57.4, 55.3, 55.2 ppm.

4.1.9.10(±)-2-((4-nitrophenyl)sulfonamido)-3-(6-((4-carbamimidoylbenzyl)oxy)naphthalen-2-yl)propanoic acid·HCl（***LX28***）

It was obtained as a light yellow solid in 38% yield. m.p. 188-191℃; HRMS (ESI): m/z, calculated for $C_{27}H_{24}N_4O_7S$, 549.1560 $(M+H)^+$, found 549.1568; ^{1}H-NMR (300MHz, DMSO-d_6): δ 9.38~9.26 (m, 4H, NH=C-NH_2 and –SO_2-NH-), 8.15~7.00 (m, 14H, Ar-H), 5.35~5.13 (m, 2H, -CH_2-O-), 4.77~4.66 (m, 1H, -CH_2-CH-NH-), 3.25~2.98 (m, 2H, -CH_2-CH-NH-); ^{13}C-NMR (75MHz, DMSO-d_6): δ 170.8, 165.1, 155.1, 144.5, 143.6, 140.1, 133.3, 130.5, 129.1, 128.7, 128.6, 128.4, 128.2, 127.9, 127.7, 127.3, 127.1, 126.5, 126.0, 124.0, 123.9, 123.4, 118.6, 108.3, 61.6, 55.9, 18.5 ppm.

4.1.9.11(±)-2-((4-bromophenyl)sulfonamido)-3-(6-((4-carbamimidoylbenzyl)oxy)naphthalen-2-yl)propanoic acid·HCl（***LX29***）

It was obtained as a yellow solid in 42% yield. m.p. 184-186℃; HRMS (ESI): m/z, calculated for $C_{27}H_{24}BrN_3O_5S$, 582.0811 $(M+H)^+$, found 582.0832; ^{1}H-NMR (300MHz, DMSO-d_6): δ 9.47~9.31 (m, 4H, NH=C-NH_2 and $-SO_2$-NH-), 7.90~7.04 (m, 14H, Ar-H), 5.34~5.25 (m, 2H, -CH_2-O-), 4.80~4.55 (m, 1H, $-CH_2$-CH-NH-), 3.05~2.82 (m, 2H, -CH_2-CH-NH-); ^{13}C-NMR (75MHz, DMSO-d_6): δ 173.5, 172.2, 151.1, 131.7, 127.4, 124.5, 112.0, 109.6, 102.0, 63.1, 52.8, 51.7, 49.0, 41.9, 36.8, 27.1, 18.5, 13.4 ppm.

4.1.9.12(±)-2-(butylsulfonamido)-3-(6-((4-carbamimidoylbenzyl)oxy)naphthalen-2-yl)propanoic acid·HCl（***LX30***）

It was obtained as a light yellow solid in 43% yield. m.p. 197-199℃; HRMS (ESI): m/z, calculated for $C_{25}H_{29}N_3O_5S$, 484.1938 $(M+H)^+$, found 484.1948; ^{1}H-NMR (300MHz, DMSO-d_6): δ 9.47~9.31 (m, 4H, NH=C-NH_2 and $-SO_2$-NH-), 7.92~7.20 (m, 14H, Ar-H), 5.36~5.27 (m, 2H, -CH_2-O-), 4.77~4.45 (m, 1H, $-CH_2$-CH-NH-), 3.05~2.82 (m, 2H, -CH_2-CH-NH-), 1.63~1.40 (m, 2H, -CH_2-CH_2-CH_2-CH_3), 1.27~1.08 (m, 2H, $-CH_2$-CH_2-CH_2-CH_3), 1.01~0.81 (m, 2H, $-CH_2$-CH_2-CH_2-CH_3), 0.58~0.56 (m, 2H, $-CH_2$-CH_2-CH_2-CH_3); ^{13}C-NMR (75MHz, DMSO-d_6): δ 175.0, 173.2, 167.7, 165.8, 155.5, 142.8, 134.3, 132.8, 129.0, 127.6, 126.4, 118.6, 107.3, 68.6, 65.3, 59.2, 58.0, 52.0, 50.7, 48.6, 31.0, 27.8, 24.9, 20.7, 13.2 ppm.

4.2 Biology

All animal experiments were handled according to the Animal Ethics Committees of the Institute of Materia Medica, Chinese Academy of Medical Sciences. The animal protocol was approved by and carried out according to the Institutional Animal Care and use Committee of China Pharmaceutical University.

Antiplatelet aggregation assays

Platelet aggregation was measured at 37°C in a platelet aggregometer (PRECILBY-NJ4，Pu Lisheng Corp.; Beijing, China) performed in Human platelet-rich plasma (PRP) was obtained by purchasing apheresis platelets from Jiangsu Province Blood Center. Platelet poor plasma (PPP) was prepared by further centrifugation at 3000r/min for 10 min, removed with a pipet and used in the reference cell of the aggregometer. Test substances dissolved in saline or 0.2% aqueous DMSO were

added to PRP to a final volume of 300ul and allowed to incubate for 1 min followed by the addition of an inducer (10 μM ADP, 1 U/ml thrombin, 6 μM U46619 or 9 μg/ml collagen) to initiate aggregation. Maximal platelet aggregation (MPA) was defined as the maximal percent increase in light transmission after addition of ADP related to the light transmission in PPP. The maximal gradient of platelet aggregation was defined as the maximal percent increase within the first 5 min. The data were obtained in triplicates.

Inhibition of antiplatelet aggregation = $\frac{PARcontrol-PARsample}{PARcontrol}$ × 100% (*PAR*: platelet aggregation ratio)

Calculation of IC_{50}

For each series of experiments in which the compounds were tested in, at least four concentrations were chosen and a percentage inhibition-concentration curve was derived. From this curve the IC_{50} value was calculated as the concentration of inhibitor causing a 50% inhibition of the aggregation using SPSS software.

Fibrinogen/GPIIb/IIIa enzyme-linked immunosorbent assay

Tissue culture-treated flat-bottom polystyrene 96-wells plates were coated with fibrinogen (10 μg/ml), diluted in 0.1 M sodium carbonate, pH 9.5 at 4℃ overnight. After unbound proteins were removed by washing with TACTS (20 mM Tris, 0.15 M NaCl, pH 7.5, 2 mM $CaCl_2$, 0.05% Tween 20) wells were blocked with 1% BSA in TACTS for 1 h. The purified human platelet GPIIb/IIIa (50μl, 20 μg/ml in TACTS) (Enzyme Research Laboratories, Southbend, IN, USA), diluted in TACTS containing 0.5% BSA, were added to the wells; then, Samples were added. After 2 h incubation, wells were washed three times with TACTS followed by addition of goat antihuman integrin β3 antibody (1:2,000, CBL479; Millipore, Bedford, MA, USA) in TACTS containing 0.5% BSA. Following 1h incubation at 37°C, wells were washed (TACTS) and anti-goat IgG conjugated alkaline phosphatase (1:1,000, A3562; Sigma) in TACTS containing 0.5% BSA was added to the wells. Before adding the stabilized *p*-nitrophenyl phosphate liquid substrate (N7653; Sigma), wells were washed three times with TACTS. After 30 min of substrate conversion, the reaction was stopped with 3 M NaOH, and absorbance was read at 405 nm using a Thermomax microplate reader (Molecular Devices). Net specific binding was obtained by subtracting optical density values from wells coated only with BSA from the total binding measured as described above. Binding was not detected in the absence of GPIIb/IIIa. All experiments were performed in triplicate.

Bleeding time assay

The bleeding time was measured by a tail transection method. Briefly, ICR mice pretreated with 3 mg/kg, 1 mg/kg, 0.3 mg/kg **LX14**, 1 mg/kg **Tirofiban** or saline 30 min before the experiments, then, mice were anesthetized intraperitoneal (i.p.) administration of 5% chloral hydrate and placed on a heating pad to maintain a constant body temperature of 37℃. A 3-mm piece of the tail-tip was cut off with a sharp scalpel. The tail was immersed into physiologic saline solution preheated to 37℃ and the time until cessation of bleeding for more than 5s was recorded.

In vivo antithrombotic study by rat arteriovenous shunt thrombosis model

SD rats (both sexes，180~220 g) were used for as rat arteriovenous shunt thrombosis model according to the method. Rats were treated by tail vein injection administration of 1 mg/kg **Tirofiban** and 0.3 mg/kg, 1 mg/kg and 3 mg/kg **LX14**. After 15 min administration of samples by tail vein injection, Rats were anesthetized by intraperitoneal (i.p.) administration of 10% chloral hydrate (3 ml/kg). The left jugular vein and right common carotid artery were isolated and catheterised by a shunt catheter (American Health & Medical Supply International Corp., Scarsdale, NY, USA). This catheter is composed of three parts including two 4 cm long polyethylene (PE) 60 catheters, which were introduced into the blood vessels, and a 12 cm long PE160 catheter that is in the middle of the two PE60 catheters. A rough silk thread (10 cm in length) was in the middle PE160 catheter to induce thrombosis. The shunt was opened for 20 min and then closed. Silk strings were removed from the middle PE160 catheter; Then, the dry weight of thrombus was weighed by drying the thrombus at 60℃ for 20 min and removing the cotton thread weigh.

4.3 Docking studies

The binding modes for the ligands to GPIIb/IIIa were generated by CDOCKER in Discovery Studio 3.0 (Accelrys Software Inc.). In CDOCKER, random ligand conformations were generated through molecular dynamics, and a variable number of translations/rotations were applied to each conformation to generate low-energy orientations of the ligand within the active site of rigid receptor. Final ligand conformations were sorted by CHARMm energy (interaction energy plus ligand strain). The crystal structures of GPIIb/IIIa (PDB entry code: 2VDM) were extracted from the Protein Database. All ligands were docked in all possible stereoisomeric forms in an active site located sphere with 12Å radius for GPIIb/IIIa, which was generated with the CreateSphere function around the subsequently removed crystal structure ligand. A total of 30 dockings for each ligand were performed, and the conformers with the lowest CHARMm energy were chosen for interpreting the docking results.

4.4 Molecular Dynamic Simulations

MD simulation of GPIIb/IIIa receptor bound to molecular LX2421 was performed using PMEMD module of AMBER 12 with ff99SB modifications [25] of the Cornell et al. force field [26]. TIP3P water molecules were applied to solvate the complex, extending 12 Å away from the protein atom. The counterions were added to the solvent to keep the system neutral. The geometry of the system was minimized before MD simulation. The whole system was heated from 0 to 300 K running 50 ps molecular dynamics with position restraints at constant volume. Subsequent isothermal isobaric ensemble (NPT)-MD was performed for 500 ps to adjust the solvent density followed by 500 ps of constant pressure equilibration at 300K without constraints to relax the system. The production dynamics at constant pressure achieved lengths of 40 ns of which snapshots saved at 20 ps intervals. The "ptraj" tool in Amber 12 was used to analyze the time-dependence of the RMSD of the Cα atoms.

Acknowledgements

This work was supported by the National Natural Science Foundation of China (81273375), China Pharmaceutical University. The authors declare no other conflicts of interest.

References

[1] Z.L. Xie, C. Cao, S. Feng, J. Huang, Z.Y. Li, Progress in the research of GPIIb/IIIa antagonists, *Future. Med. Chem.* 7 (2015) 1149-1171.

[2] A. Garg, A. Pandey, P. Oza, M. Chaturvedi, Newer anti-platelet and anti-thrombotic drugs on the horizon, *Nat. J. Physio. Pharm. & Pharmaco*. 3 (2013) 105-110.

[3] H.D. Park, S.H. Lee, T.H. Kim, S.H. Lee, H. Hyung, Antithrombotic effects of LB30870, a potent, orally active, selective and direct thrombin inhibitor, and pharmacokinetics of its prodrug, *Bioorg. Med. Chem. Lett.* 23 (2013) 4779-4784.

[4] D.M. Alan, Antiplatelet therapies for the treatment of cardiovascular disease, *Nat. Rev. drug. Discov.* 9 (2010) 154-169.

[5] A. Karolina, A. Dimitrios, Use of antiplatelet agents in sepsis: A glimpse into the future, *Thromb. Res.* 133 (2014) 131-138.

[6] X.L. Ying, S. Qiang, Z. Hui *et al*, A novel anti-platelet peptide (Z4A5) potential for glycoprotein IIb/IIIa inhibits platelet aggregation, *Thromb. Res.* 129 (2012) 217-222.

[7] S.T. Udaya, G. Martin, L. Fang, P.B. Kevin, A.G. Paul, Resistance to antiplatelet drugs: what progress has been made, *Expert Opin. Pharmacother*. 15(2014) 2553-2564

[8] C.E. Hagemeyer, K. Peter, Targeting the Platelet Integrin GPIIb/IIIa, *Curr. Pharm. Design*. 16 (2010) 4119-4133.

[9] G.P. Pavel, V.S. Georgiy, M.K. Tetiana, L.K. Olga, A.K. Tatyana, M.K. Vladimir, Y.K. Alexander, K. Olga, L. Thierry, A.A. Sergei, E.K. Victor, A.K. Andrei, V. Alexandre, Design, Virtual Screening, and Synthesis of Antagonists of αIIbβ 3 as Antiplatelet Agents, *J. Med. Chem*. 58 (2015) 7681-7694.

[10] M. Ilic, P. Dunkel, J. Ilas, E. Chabielska, A. Zakrzeska, P. Mátyus, D. Kikelj, Towa rds dual antithrombotic compounds e Balancing thrombin inhibitory and fibrinogen GPIIb/IIIa binding inhibitory activities of 2,3-dihydro-1,4-benzodioxine derivatives through regio- and stereoisomerism, *Eur. J. Med. Chem*. 62 (2013) 329-340.

[11] U. Trstenjak, J. Ila, D. Kikelj, Low molecular weight dual inhibitors of factor Xa and fibrinogen binding to GPIIb/IIIa with highly overlapped pharmacophores, *Eur. J. Med. Chem.* 64 (2013) 302-313.

[12] A.K. Andrei, V.S. Georgiy, G.P. Pavel, S.F. Marina, C.K. Victor, A.A. Sergei, A.K. Tatyana, L. Janusz, M.K. Tetiana, E.K. Victor, M.K. Vladimir, L.K. Olga, A.V. Alexandre, Synthesis, biological evaluation, X-ray molecular structure and molecular docking studies of RGD mimetics containing 6-amino-2,3-dihydroisoindolin-1-one fragment as ligands of integrin αIIbβ3, *Bioorg. Med. Chem.* 21 (2013) 4646-4661.

[13] C.A. Paul, P. Karlheinz, GPIIb/IIIa inhibitors: From bench to bedside and back to bench again, *Thromb. Haemostasis.* 107 (2012) 808-814.

[14] J.Q. Zhu, J.H. Zhu, A. Negri, D. Provasi, M. Filizola, B.S. Coller, T.A. Springer, Closed headpiece of integrin αIIbβ3 and its complex with an αIIbβ3-specific antagonist that does not induce opening, *Blood*. 116 (2010) 5050-5059.

[15] S.N. Nancy, A.A. Norman, G.P. Susan, G.F. Leo, D.P. Jimmy, K.S. Anita, D.S. Osman, A.S. James, B.T. Beatrice, J.A. Robert, Orbofiban : An Orally Active GPIIb/IIIa Platelet Receptor Antagonist, *Med. Res. Rev.* 21(2001) 211-226.

[16] A.B. Michelle, A.J. Joseph, S. Atsuhiro, R.B. Marc, D.M. Alan, L.F. Andrew, P2Y12 Receptor Blockade Augments Glycoprotein IIb-IIIa Antagonist Inhibition of Platelet Activation, Aggregation, and Procoagulant Activity, *J. Am. Heart. Assoc*. 2(2013) 1-10.

[17] N. Ana, L. Jihong, N. Sarasija, S.C. Barry, F. Marta, Structure-based virtual screening of small-molecule antagonists of platelet integrin αIIbβ3 that do not prime the receptor to bind ligand, *J. Comput. Aided. Mol. Des.* 26 (2012) 1005-1015.

[18] A. Negri, J. Li, S. Naini, B.S. Coller, M. Filizola, Structure-based virtual screening of small-molecule antagonists of platelet integrin aIIbβ3 that do not prime the receptor to bind ligand, *J. Comput. Aided. Mol. Des*. 26 (2012) 1005-1015.

[19] L. Chang, L.T. Jia, Y.X. Si, F.L. Jie, R.Z. Guang, X.A. Xi, B.C. Jian, X. Yi, Y. Quan, Z. Hua,

1,4-Benzoxazine-3(4H)-ones as Potent Inhibitors of Platelet Aggregation: Design, Synthesis and Structure–Activity Relations, *Chem. Pharm. Bull.* 62(2014) 915–920.

[20] L. Alessandro, R. Andrea, P. Italo, TCT-843 Drug eluting balloon vs drug eluting stent in PCI: insights from a meta-analysis of 1462 patients, *J. Am. Coll. Cardiol.* 62 (2013) 254-254.

[21] Y. Kong, J.L. Huo, W. Xu, J. Xiong, Y.M. Li, W.T. Wu, A novel anti-platelet aggregation tripeptide from Agkistrodon acutusvenom: Isolation and characterization, *Toxicon*. 54 (2009) 103-109.

[22] J. Xiong, L. Bai, W. Fang, J.Y. Fu, W. Fang, J. Cen, Y. Kong, Y.M. Li, New peptide pENW (pGlu-Asn-Trp) inhibits platelet activation by attenuating Akt phosphorylation, *Eur. J. Pharm. Sci*. 45 (2012) 552-558.

[23] Z.L. Xie, S. Feng, Y. Wang, C. Cao, J. Huang, Y.H. Chen, Y. Kong, Z.Y. Li, Design, synthesis of novel tryptophan derivatives for antiplatelet aggregation activity based on tripeptide pENW (pGlu-Asn-Trp), *Eur. J. Med. Chem*. 102 (2015) 363-374.

[24] A.V. Marco, R. F. Frank, W.H. Gregory, L.M. Mark, Syntheses of 1- and 2-Naphthol Analogues of DL-Tyrosine. Potential Fluorescent Probes of Peptide Structure and Dynamics in Complex Environments, *J. Org. Chem.* 55 (1990) 2913-2918.

[25] C. Simmerling, B. Strockbine, A.E. Roitberg, All-atom structure prediction and folding simulations of a stable protein, *J. Am. Chem. Soc.* 124 (2002) 11258-11259.

[26] W.D. Cornell, P. Cieplak, C.I. Bayly, I.R. Gould, K.M. Merz, D.M. Ferguson, D.C. Spellmeyer, T. Fox, J. W. Caldwell, P.A. Kollman, A Second Generation Force Field for the Simulation of Proteins, Nucleic Acids, and Organic Molecules, *J. Am. Chem. Soc.* 117(1995) 5179-5197.

Figure caption

Fig. 1. The mechanism of platelet aggregation and some representing drugs of antiplatelet aggregation.

Fig. 2. (A) The docking model of LX2421 with GPIIb/IIIa receptor, the figure was prepared by Discovery Studio 3.0. (For interpretation of the references to color in this figure legend, the reader is referred to the web version of this article.). (B) The key interactions formed between LX2421 and GPIIb/IIIa along the MD trajectories. The key interactions of which occupancies were more than 40% were considered and shown in the figure. The key interactions are colored as red (occupancy greater than 80%), purple (occupancy of 60−80%), blue (occupancy of 40−60%).

Fig. 3. The identification of novel compound LX5.

Fig. 4. The activity of LX14 (A, B, C) and LX25 (D, E, F) for inhibiting Collagen (1μg/ml) Thrombin (0.26 U/ml) and U46619 (2 μM)-induced human platelet aggregation. The activity was shown as an inhibition ratio to control group. Data are expressed as mean ± SD (n=3).

Fig. 5. The GPIIb/IIIa receptor inhibitory activities of LX14 and LX25 in comparison with Tirofiban in the fibrinogen/GPIIb/IIIa enzyme-linked immunosorbent assay. Data are expressed as mean ± SD (n=3).

Fig. 6. Docking mode of LX14 (A) and LX25 (B) binding to GPIIb/IIIa receptor in comparison with Tirfiban, figure A: compound LX14 (purple, bold), Tirofbian (brown, thin); figure B: compound LX25 (blue). (For interpretation of the references to color in this figure legend, the reader is referred to the web version of this article.).

Fig. 7. Bleeding time induced by intravenous injection of compound LX14 (3, 15, and 30 mg/kg) and Tirofiban (1 mg/kg). The accumulated bleeding time was recorded within 20 min. Data are expressed as mean ± SD (n= 6). *P < 0.05, ****P < 0.0001 compared with control group, #P < 0.01 compared with Tirofiban-treated group.

Fig. 8. The antithrombotic activities of compound LX14 and Tirofiban in vivo in the rat arteriovenous shunt thrombosis model. Three doses were tested for LX14 (1, 5 and 10 mg/kg), and one dose (1 mg/kg) was tested for Tirofiban. Data are expressed as mean ± SD (n= 6). *P < 0.05, ****P < 0.0001 compared with control group.

Scheme caption

Scheme 1. *Conditions and reagents*: **a**) RCl , K_2CO_3, acetone/water (v:v=1:2), 65℃, overnight, 80-88%; **b**) LiOH, acetone/ methanol/water (v:v:v=1:1:1), 50 ℃ , overnight, 75-89%; **c**) 1-Boc-4-(methylsulfonyl)oxy)propyl)piperidine or 1-Boc-4-(2-((methylsulfonyl)oxy)propyl)piperidine or 1-Boc-4-(2-((methylsulfonyl)oxy)propyl)piperidine or 1-Boc-4-(3-((methylsulfonyl)oxy)propyl)piperidine or 1-Boc-4-(4-((methylsulfonyl)oxy)butyl)piperidine, K_2CO_3, DMF, N_2, 80℃, 12 h, 42-48%; **d**) HCl (g), AcOEt, -5 ℃, 4h, 82-90%; **e**) $SOCl_2$, methanol, 50 ℃, 6 h, 95%; **f**) $Br(CH_2)_nBr$, K_2CO_3, dry acetonitrile, 60℃, 48 h, 35-50%; **g**) *N*-Boc-piperazine, K_2CO_3, dry acetonitrile, 60℃, 48 h, 30-60%; **h**) LiOH•H_2O, MeOH/THF/H_2O (v:v:v=1:1:1), r.t., 5 h, 40-55%; **i**) HCl(g), AcOEt, 0℃, 4 h, 90-95%. **j**) 4-CNPh-CH_2Br (1.5 equiv.)/K_2CO_3 (2.0 equiv.), dry acetonitrile, reflux, overnight, 60%~70%; **k**) HCl/MeOH, NH_3/MeOH, -5℃, overnight, 45%~50%; **l**) LiOH•H_2O, MeOH/THF/H_2O (v:v:v=1:1:1), r.t., overnight, 65-68%.

Table 1 Antiplatelet aggregation activity of naphthalene derivatives LX1-LX6 designed from LX2421.

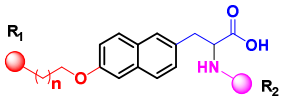

Compound	R_1	R_2	n	Inhibition%/50μM[a]	IC_{50}(μM)[b]
LX1			0	<5.00	>100
LX2			1	<5.00	>100
LX3			2	<5.00	>100
LX4			1	97.3±1.6	12.8±1.04
LX5			2	99.1±2.3	0.37±0.03
LX6			3	91.2±2.4	18.8±1.12
2421				38.1±1.8	ND[c]

[a] In vitro inhibition of ADP-induced (20 μM) human platelet aggregation; See the Experimental Section for details; the data represent the mean of at least three independent determinations.

[b] In vitro inhibition of ADP-induced (20 μM) human platelet aggregation; See the Experimental Section for details; Values are means from two to three independent dose–response curves.

[c] ND means not determined.

Table 2 Antiplatelet aggregation activity of naphthalene derivatives LX19-LX30 designed from LX5.

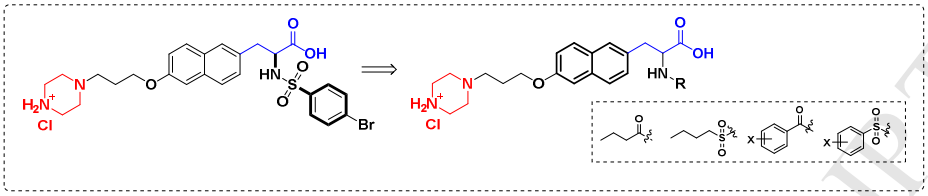

Compound	R	IC_{50}(μM)[a]	Compound	R	IC_{50}(μM)[a]
LX7		7.90±2.11	**LX13**		5.40±0.04
LX8		6.38±1.05	**LX14**		0.18±0.07
LX9		7.60±1.54	**LX15**		0.28±1.12
LX10		24.60±1.98	**LX16**		0.20±0.08
LX11	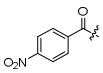	3.40±0.06	**LX17**	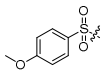	1.65±1.01
LX12	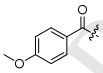	12.70±1.62	**LX18**		0.52±0.04
LX2421		ND[b]	**Tirofiban**		0.09±0.03

[a] In vitro inhibition of ADP-induced (20 μM) human platelet aggregation; See the Experimental Section for details; Values are means from two to three independent dose–response curves.

[b] ND means not determined.

Table 3 Antiplatelet aggregation activity of naphthalene derivatives LX19-LX30 designed from LX5.

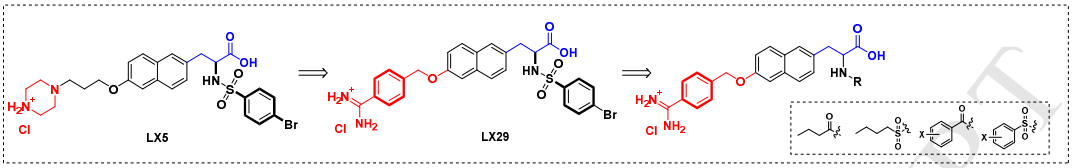

Cpd	R	Inhibition%/ 50μM[b]	IC_{50}(μM)[a]	Cpd	R	Inhibition%/ 50μM[b]	IC_{50}(μM)[a]
LX19		49.4±2.3	ND[c]	**LX25**		>99.5	0.84±0.09
LX20		49.7±0.8	ND	**LX26**		>99.5	4.01±2.31
LX21		23.3±4.1	ND	**LX27**	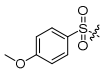	21.5±1.5	ND
LX22	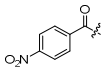	>99.5	2.10±1.22	**LX28**	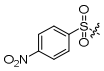	62.9±2.7	ND
LX23	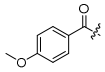	32.4±3.9	ND	**LX29**		50.2±3.4	ND
LX24		>99.5	1.08±0.06	**LX30**		>99.5	3.29±1.07
LX2421			ND	**Tirofiban**			0.09±0.03

[a] In vitro inhibition of ADP-induced (20 μM) human platelet aggregation; See the Experimental Section for details; Values are means from two to three independent dose–response curves.

[b] In vitro inhibition of ADP-induced (20 μM) human platelet aggregation; See the Experimental Section for details; The data represent the mean of at least three independent determinations.

[c] ND means not determined.

Table 4 The activity of LX14 and LX25 for inhibiting ADP (20 μM), Collagen (1μg/ml), Thrombin (0.26 U/ml) and U46619 (2 μM)-induced human platelet aggregation.

LX14		**LX25**	
Inducer	**IC_{50} (μM)[a]**	**Inducer**	**IC_{50} (μM)[a]**
ADP (20 μM)	0.18±0.07	ADP (20 μM)	0.84±0.09
COLL (1 ug/ml)	1.32±0.09	COLL (1 ug/ml)	27.7±1.67
Thr (0.26 U/ml)	0.53±0.14	Thr (0.26 U/ml)	22.9±2.12
U46619 (2 μM)	1.01±0.26	U46619 (2 μM)	23.6±2.07

[a] Values are means from two to three independent dose–response curves.

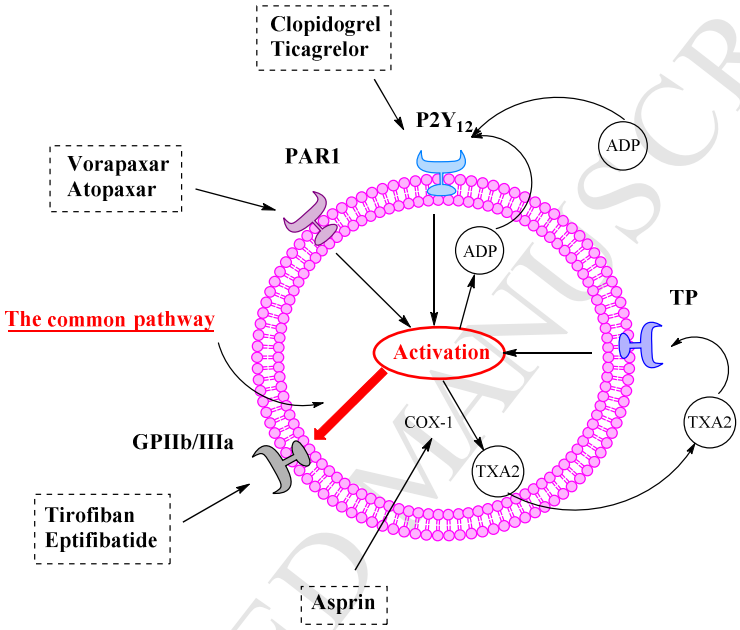

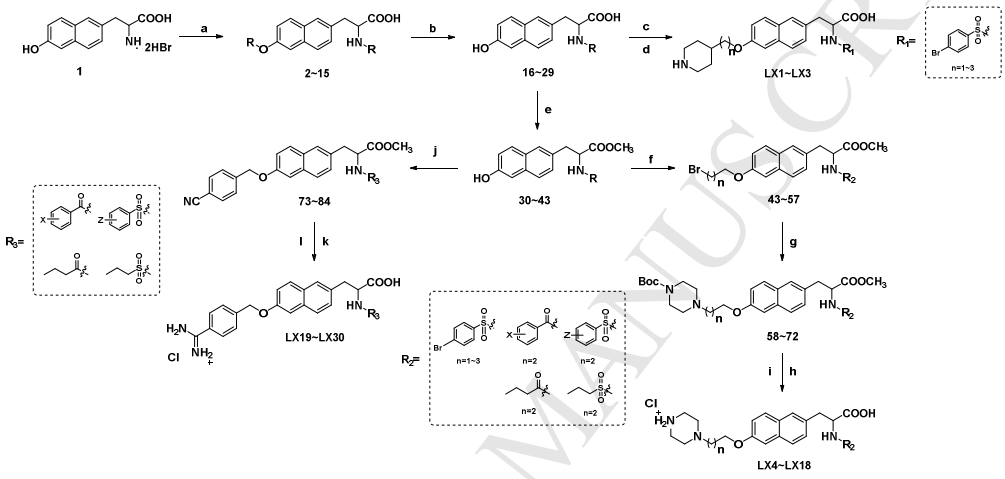

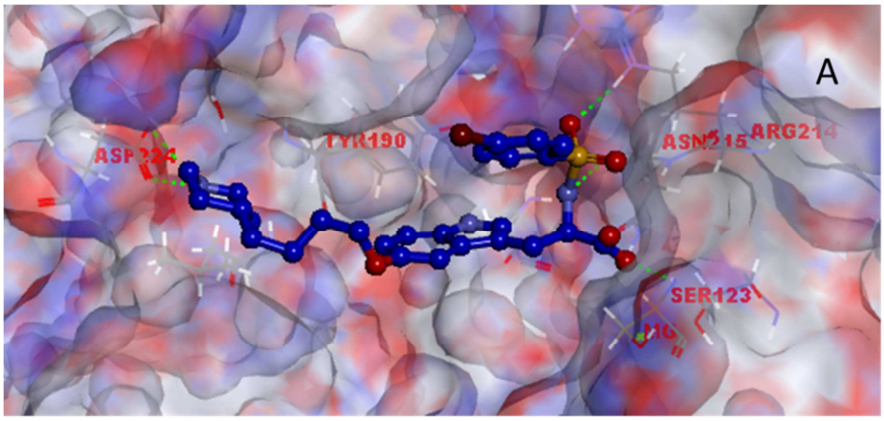

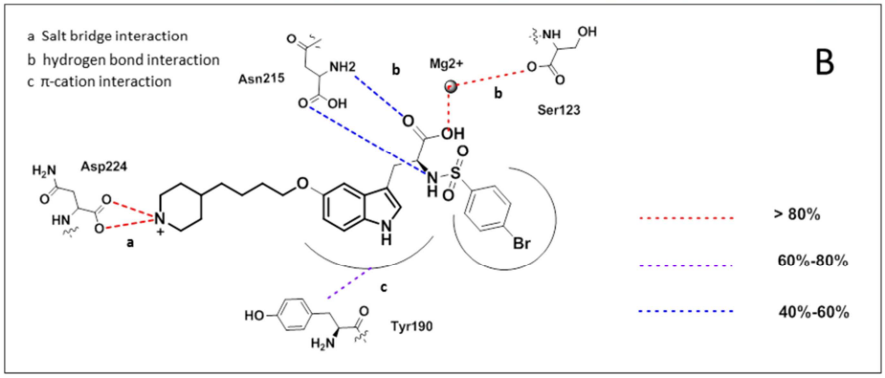

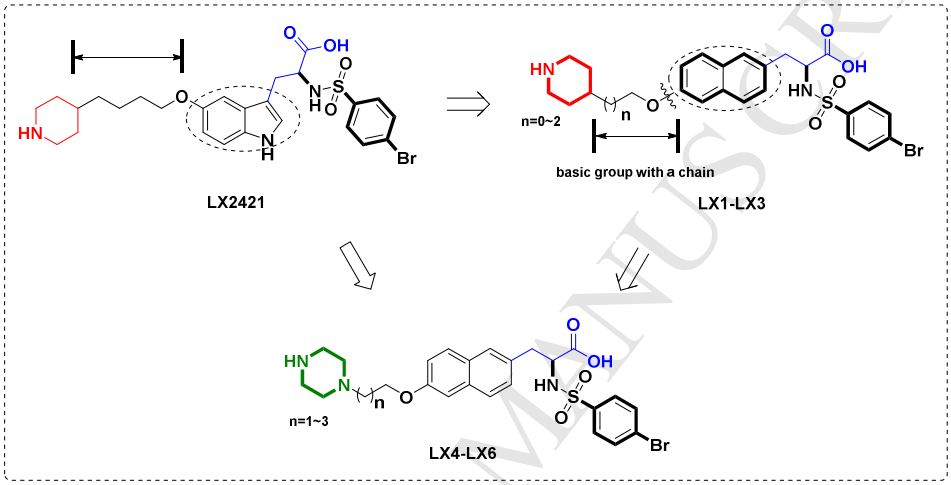

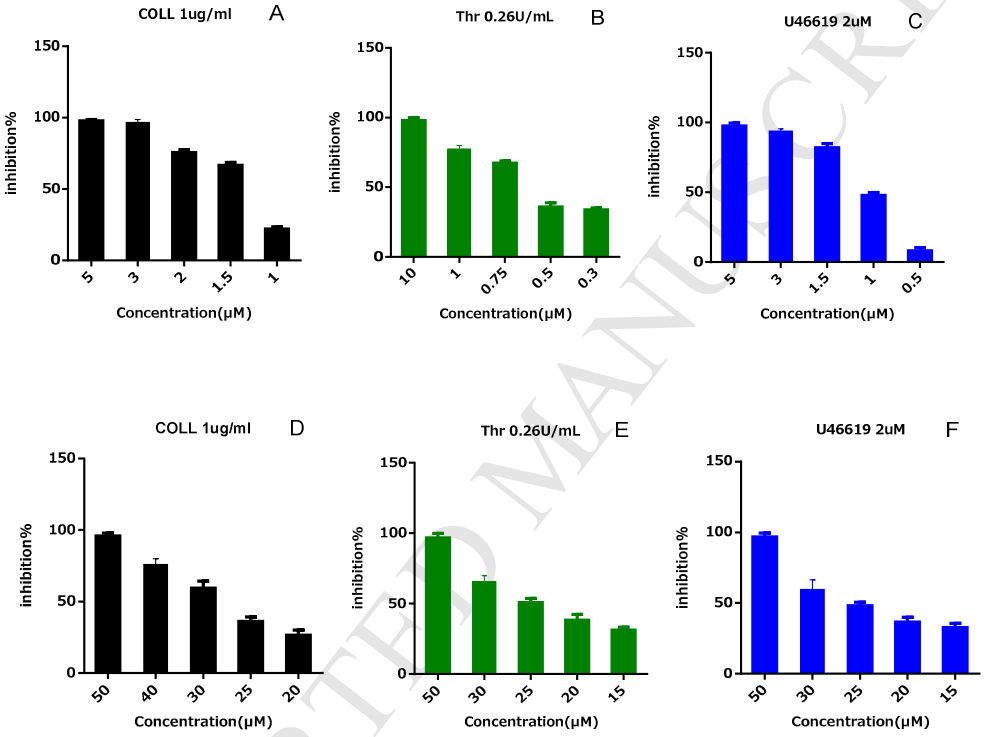

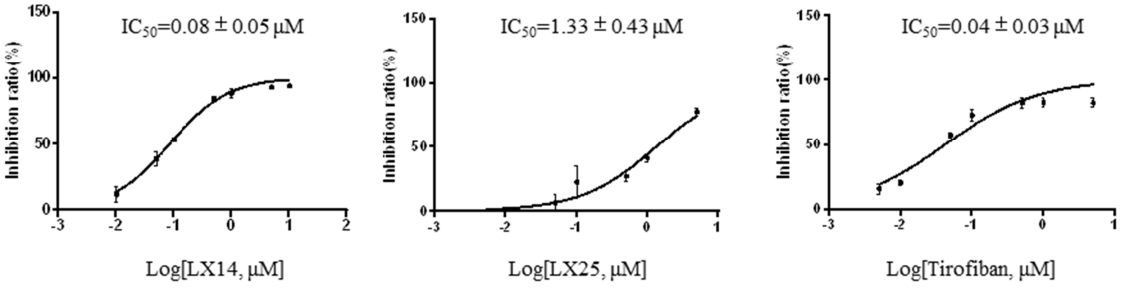

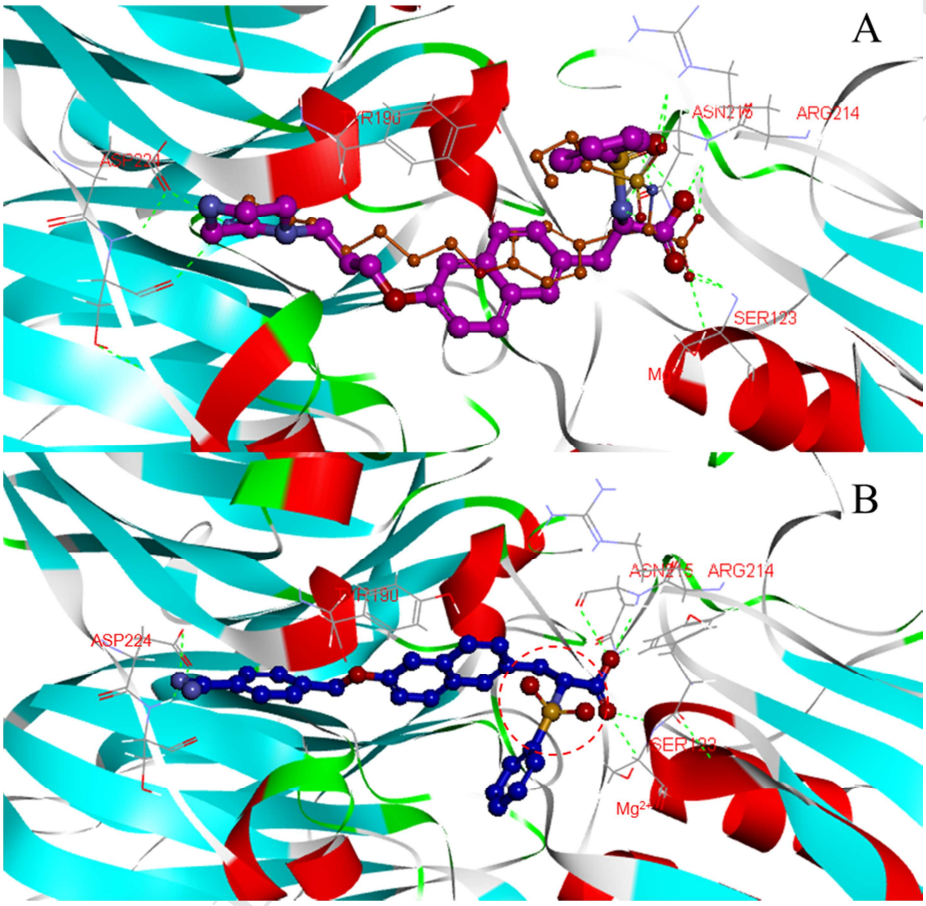

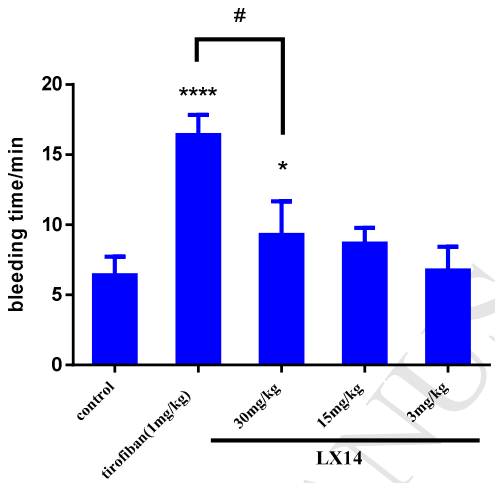

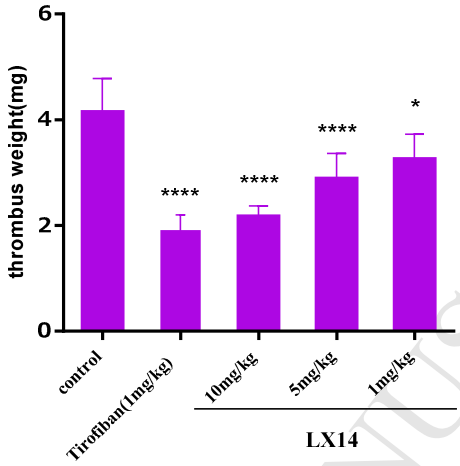

Highlights:

- **LX5** was identified based on an identified antiplatelet aggregation agent **LX2421**.
- A series of 2-amino-3-(naphth-2-yl)propanoic acid derivatives were synthesized and evaluated for antiplatelet aggregation activity.
- **LX14** shows comparable ability as **Tirofiban** in inhibiting platelet aggregation and GPIIb/IIIa receptor.
- **LX14** has less bleeding risk in comparison with **Tirofiban**.